Novel genetic basis of resistance to Bt toxin Cry1Ac in *Helicoverpa zea*

Kyle M. Benowitz[1,2,*], Carson W. Allan[1], Benjamin A. Degain[1], Xianchun Li[1], Jeffrey A. Fabrick[3], Bruce E. Tabashnik[1], Yves Carrière[1], Luciano M. Matzkin[1,4,5]

[1]Department of Entomology, University of Arizona, Tucson, AZ, USA

[2]Department of Biology, Austin Peay State University, Clarksville, TN, USA

[3]U.S. Department of Agriculture, Agricultural Research Service, U.S. Arid Land Agricultural Research Center, Maricopa, AZ, USA

[4]Department of Ecology and Evolutionary Biology, University of Arizona, Tucson, AZ, USA

[5]Bio5 Institute, University of Arizona, Tucson, AZ, USA

Corresponding author: Kyle M. Benowitz. Department of Biology, Austin Peay State University, Sundquist Science Center, PO Box 4718, Clarksville, TN 37044. Email: benowitzk@apsu.edu

Running Title: *Novel genetic basis of Bt resistance*

Abstract

Crops genetically engineered to produce insecticidal proteins from the bacterium *Bacillus thuringiensis* (Bt) have advanced pest management, but their benefits are diminished when pests evolve resistance. Elucidating the genetic basis of pest resistance to Bt toxins can improve resistance monitoring, resistance management, and design of new insecticides. Here, we investigated the genetic basis of resistance to Bt toxin Cry1Ac in the lepidopteran *Helicoverpa zea*, one of the most damaging crop pests in the United States. To facilitate this research, we built the first chromosome-level genome assembly for this species, which has 31 chromosomes containing 375 Mb and 15,482 predicted proteins. Using a genome-wide association study, fine-scale mapping, and RNA-seq, we identified a 250-kb quantitative trait locus (QTL) on chromosome 13 that was strongly associated with resistance in a strain of *H. zea* that had been selected for resistance in the field and lab. The mutation in this QTL contributed to but was not sufficient for resistance, which implies alleles in more than one gene contributed to resistance. This QTL contains no genes with a previously reported role in resistance or susceptibility to Bt toxins. However, in resistant insects, this QTL has a premature stop codon in a kinesin gene which is a primary candidate as a mutation contributing to resistance. We found no changes in gene sequence or expression consistently associated with resistance for 11 genes previously implicated in lepidopteran resistance to Cry1Ac. Thus, the results reveal a novel and polygenic basis of resistance.

Keywords: *Bacillus thuringiensis*; genome wide association study; genome assembly; insecticide resistance; kinesin; Lepidoptera; transgenic crops

Introduction

Crops genetically engineered to produce insecticidal proteins from *Bacillus thuringiensis* (Bt) have provided control of some key pests during the past 25 years while reducing insecticide sprays and conserving arthropod natural enemies (Bravo *et al.* 2011; NASEM 2016; Dively *et al.* 2018; Romeis *et al.* 2018; Carrière *et al.* 2020a; Tabashnik *et al.* 2021). However, planting of a cumulative total of more than one billion hectares of Bt crops worldwide (ISAAA 2019) has selected for resistance that has reduced the efficacy of Bt crops against populations of at least nine major pest species (Calles-Torrez *et al.* 2019; Smith *et al.* 2019; Tabashnik and Carrière 2019). Knowledge of the genetic basis of pest resistance to Bt toxins can be useful for improving monitoring and management of resistance, as well as for designing new insecticides (Soberón *et al.* 2007; Jin *et al.* 2018).

Resistance to crystalline (Cry) Bt toxins typically entails mutations that reduce binding of the toxins to larval midgut receptors and thus block an essential step in the mode of action (Heckel *et al.* 2007; Peterson *et al.* 2017; Jurat-Fuentes *et al.* 2021). In particular, research has repeatedly implicated disruption or reduced expression of known or putative Bt toxin receptors from four protein families: ATP-binding cassette (ABC), cadherin, aminopeptidase N (APN), and alkaline phosphatase (ALP). Mutations that disrupt binding of toxins to receptors are frequently associated with high levels of resistance to one or a few closely related Bt toxins, weak or no cross-resistance to unrelated Bt toxins, and recessive inheritance of resistance (Mode 1 resistance; Tabashnik *et al.* 1998). Nonetheless, lepidopteran resistance to Bt toxins also includes examples where proteins from these families are not involved, toxin binding is not reduced, and inheritance of resistance is not recessive (Peterson *et al.* 2017; Jin *et al.* 2018).

Here we analyzed the genetic basis of resistance to Bt toxin Cry1Ac in the lepidopteran *Helicoverpa zea* (corn earworm or bollworm), which is one of the most economically important crop pests in the United States (Cook and Threet 2019; Musser *et al.* 2019). This polyphagous pest is the first insect reported to have evolved resistance to a Bt crop, specifically to cotton producing Cry1Ac (Luttrell *et al.* 1999; Ali *et al.* 2006; Tabashnik *et al.* 2008; Reisig *et al.* 2018). In contrast with Mode 1 resistance, inheritance of resistance to Cry1Ac in *H. zea* is not completely recessive (Brévault *et al.* 2013, 2015; Carrière *et al.* 2020b; Reisig *et al.* 2021).

Caccia *et al.* (2012) concluded that resistance in their lab-selected AR1 strain of *H. zea* was complex, possibly polygenic, and not caused primarily by reduced binding of Cry1Ac to larval midgut membranes. Perera *et al.* (2021) found that knocking out the gene encoding the putative Cry1Ac receptor ABCC2 increased the concentration of Cry1Ac killing 50% of larvae (LC_{50}) by 7- to 40-fold. Because >100-fold resistance to Cry1Ac is common in lab- and field-selected *H. zea* (Caccia *et al.* 2012; Brévault *et al.* 2013; Reisig *et al.* 2018; Kaur *et al.* 2019), they inferred that mutations disrupting ABCC2 are not the sole or primary mechanism of resistance to Cry1Ac in *H. zea.* Although most previous studies of Bt resistance in *H. zea* have emphasized the gene families listed above (Caccia *et al.* 2012; Zhang *et al.* 2019a; Fritz *et al.* 2020; Perera *et al.* 2021; Taylor *et al.* 2021), additional candidates have been identified using RNA-seq (Lawrie *et al.* 2020; 2022).

Our work focuses on the GA-R strain of *H. zea*, which had been selected for resistance to Bt toxins in the field and lab (Brévault *et al.* 2013, Welch *et al.* 2015). GA-R was derived from the moderately resistant GA strain, which had been selected for resistance to Bt toxins only in the field (Brévault *et al.* 2013). Relative to an unrelated susceptible lab strain (LAB-S) of *H. zea*, the LC_{50} of Cry1Ac was >500 times higher for GA-R and 55 times higher for GA (Brévault *et al.* 2013). Previous work identified reduced activation of Cry1Ac by midgut proteases as a potential field-selected mechanism of resistance that could explain part but not all of the resistance in GA-R relative to LAB-S (Zhang *et al.* 2019a). Overall, the previous results with GA-R and other strains of *H. zea* summarized above led us to hypothesize that resistance to Cry1Ac in this species is polygenic and entails novel genetic mechanisms. Accordingly, genome-wide mapping approaches are warranted, but have been hindered because the only *H. zea* genome assembly available is highly fragmented (Pearce *et al.* 2017).

Here, we generated a chromosome-level genome for *H. zea*, then used a genome wide association study (GWAS), fine-scale mapping, and RNA-seq to elucidate the genetic basis of resistance to Cry1Ac in the GA-R strain of *H. zea.* We identified a quantitative trait locus (QTL) of 250 kb on chromosome 13 that was strongly associated with resistance to Cry1Ac. The results indicate a mutation in this QTL contributed to resistance but was not sufficient for resistance in GA-R. We also found no consistent association between resistance to Cry1Ac and any of 11 genes previously implicated in lepidopteran resistance to Bt toxins. We conclude the genetic

basis of resistance to Cry1Ac in GA-R is novel and polygenic.

Materials and methods

Insect strains

We used four strains of *H. zea*: the highly resistant strain GA-R, its moderately resistant parent strain GA, the unrelated susceptible strain LAB-S, and the heterogeneous strain GA-RS that we created by crossing GA-R with LAB-S as described below. LAB-S was obtained from Benzon Research Inc. (Carlisle, PA, USA) and has not been exposed to Bt toxins or other insecticides. The resistant strain GA-R was derived from the third generation (F3) of the GA strain, which was started with 180 larvae collected on Cry1Ab corn from Tifton, Georgia in 2008 (Brévault *et al.*, 2013). GA-R was initially selected with Cry1Ac for nine generations and with MVPII thereafter (Brévault *et al.* 2013; Fritz *et al.* 2020; Carrière *et al.* 2020b). MVPII is a liquid formulation of a hybrid protoxin produced by transgenic *Pseudomonas fluorescens.* The amino acid sequence of the active portion of the protoxin is identical in the hybrid protoxin and Cry1Ac (Welch *et al.* 2015). For simplicity, hereafter we refer to MVPII as Cry1Ac. Amino acid sequence similarity between Cry1Ab and Cry1Ac is 86% (Carrière *et al.* 2015). Lab selection with Cry1Ac caused cross-resistance to Cry1Ab in GA-R (Welch *et al.* 2015) and in the AR strain of *H. zea* (Anilkumar *et al.* 2008). Moreover, adoption of Cry1Ac-producing cotton, a host plant of *H. zea*, was 94% in Georgia in 2008 (USDA 2008) and high in several preceding years (USDA 2020). Thus, the observed resistance to Cry1Ac in the GA strain (Brévault *et al.* 2013) could reflect direct selection in the field with Cry1Ac, cross-resistance from selection in the field with Cry1Ab, or both.

We conducted all rearing in walk-in growth chambers at 27 ± 1°C with 14h light: 10h dark photoperiod. We reared larvae on a casein-based wheat germ diet (Orpet *et al.* 2015a, 2015b) and conducted larval bioassays on Southland diet (Southland Products, Inc., Lake Village, AR, USA). We use these two different diets to optimize larval development and surface uniformity for toxin overlay in bioassays, respectively (Carrière *et al.* 2020b). Moths were kept in walk-in growth chambers under the same temperature and photoperiod mentioned above but under higher

relative humidity than for larvae (60% Rh for moths and 20% Rh for larvae). Moths had access to a 10% sugar water solution for feeding and cheese cloth for oviposition (Welch *et al.* 2015). As previously reported (Fritz *et al.* 2020), we reared ca. 600 moths per generation for the first 35 and 33 generations of GA and GA-R, respectively. In 2012, we crossed GA with GA-R and used the resulting progeny to continue GA-R (Carrière *et al.* 2020b). After this interstrain cross, to reduce genetic drift and inbreeding, we reared two subsets of GA and crossed the two subsets every one to three generations (Carrière *et al.* 2020b). We used the same procedure to rear and cross two subsets of GA-R. Each subset had ca. 600 moths per generation (ca. 1200 moths per strain per generation). For GA, the mean number of moths per generation for F1 to F72 was ca. 900, based on the number of moths per generation of 600 for F1-F36 and 1200 for F37-72.

Relative to GA, GA-R had significantly higher survival on Bt cotton (producing Cry1Ac, Cry1Ac + Cry2Ab, or Cry1Ac + Cry1F) and Bt corn producing Cry1A.105 + Cry2Ab (Brévault *et al.* 2013, 2015; Carrière *et al.* 2018, 2019, 2020b, 2021). At the time we crossed GA-R with LAB-S in May 2018, we had selected GA-R with Cry1Ac for 58 generations. The GA-RS strain was created using mass reciprocal crosses between GA-R and LAB-S (i.e., 120 GA-R females × 120 LAB-S males and 120 LAB-S females × 120 GA-R males). GA-RS was founded with 450 neonates from each reciprocal cross. In the founding and subsequent generations, 900 larvae were reared and 600 adults (sex ratio 1:1) produced the neonates used for propagating the next generation.

Genome sequencing of resistant strain GA-R

We generated a *de novo* genome assembly for GA-R using an approach combining a hybrid short- and long-read assembly with a long-read only assembly (Jaworski *et al.* 2020), which allows for improved error correction of long read data (Ye *et al.* 2016) without the need for massive coverage (Chakraborty *et al.* 2016). Hybrid assembly strategies have been used frequently with error-prone PacBio CLR data to generate highly contiguous genomes in non-model insect species (Hartke *et al*. 2019; Wan *et al.* 2019; Ferguson *et al*. 2020; Jaworski *et al.* 2020; Ma *et al.* 2020; Mathers 2020; Schmidt *et al.* 2020; Xu *et al.* 2021). For the short-read

assembly, we collected and sequenced 30 GA-R larvae as described below. We trimmed reads and generated the assembly using Platanus (Kajitani *et al.* 2014). For the long-read assembly, we extracted DNA from the gut of a single GA-R fifth instar using a chloroform-based extraction method (Jaworski *et al.* 2020). PacBio libraries were constructed at the Arizona Genomics Institute (Tucson, AZ, USA). We then sequenced the library on a single lane of PacBio Sequel II, also at the Arizona Genomics Institute. We formatted raw PacBio reads using bam2fastq (https://github.com/jts/bam2fastq) and SeqKit (Shen *et al.* 2016) before filtering out all reads under 30-kb using Filtlong (https://github.com/rrwick/Filtlong). We mapped contigs from the short-read assembly to the long reads using DBG2OLC (Ye *et al.* 2016) before running three iterations of Sparc (Ye and Ma 2016) to correct the resulting contigs. We realigned the raw PacBio reads to the resulting assembly with pbmm2 (https://github.com/PacificBiosciences/pbmm2) and polished contigs using Arrow (Chin *et al.* 2013; https://github.com/PacificBiosciences/GenomicConsensus). Lastly, we mapped raw short reads to the assembly with Bowtie2 (Langmead and Salzberg 2012) to perform a final polishing step using Pilon (Walker *et al.* 2014).

We generated the PacBio-only assembly with Canu (Koren *et al.* 2017), using the reads longer than 30kb after filtering described above. We then polished the assembly using Arrow and Pilon as described above. Finally, we used Purge Haplotigs (Roach *et al.* 2018) to remove contigs containing alternate haplotypes generated due to high heterozygosity.

We aligned the two assemblies using nucmer within MUMmer4 (Marçais *et al.* 2018), keeping only alignments greater than 10 kb. We then generated the merged assembly using Quickmerge (Chakraborty *et al.* 2016). We performed additional merging by re-running Quickmerge with more liberal parameters on individual contig pairs after hypothesizing their contiguity based on synteny with *H. armigera* (Pearce *et al.* 2017; Valencia-Montoya *et al.* 2020). Specifically, chromosomes 5, 7, 8, 16, 17, 18, 19, 21, 23, 29, and 30 required such additional merging. After this step, only chromosome 17 had two contigs that did not merge. We therefore connected them with a default 100-bp gap according to NCBI standards (Karsch-Mizrachi *et al.* 2012). We again polished the final assembly using Arrow, Pilon, and Purge Haplotigs as above. Lastly, we ordered and named each chromosome to align with those of *H. armigera*. We generated a synteny plot comparing our genome to the *H. armigera* genome using Dot

(https://github.com/marianattestad/dot) after filtering out alignments under 4000 bp in NUCmer.

We analyzed the completeness of the GA-R genome using BUSCO v.5 (Seppey *et al.* 2019), comparing genomic content against the lepidodptera_odb10 set of 5,286 conserved single copy genes. We calculated contig (before final merging of chromosome 17) and scaffold (final assembly) genome summary statistics with bbmap stats (https://sourceforge.net/projects/bbmap/). We calculated repeat content with RepeatModeler2 (Flynn *et al.* 2020) and RepeatMasker (Smit *et al.* 2013-2015). We provide a preliminary annotation produced following the funannotate pipeline (Palmer and Stajich 2020) with transcripts from *H. armigera* and proteins from *B. mori* used as evidence supporting putative annotations. We also used BUSCO v.5 to assess the completeness and accuracy of the annotation against the 5,286 single copy genes in the lepidoptera_odb10 dataset. To compare the quality of our assembly and annotation with the previous *H. zea* genome assembly (Pearce *et al.* 2017), we reanalyzed the genomic and proteomic BUSCO scores of that assembly against the same lepidoptera_odb10 dataset.

Phenotyping of Cry1Ac-susceptible and -resistant larvae for genetic mapping

We used our standard diet overlay bioassay (Welch *et al.* 2015) to characterize GA-RS larvae as susceptible or resistant to Cry1Ac. We added 40 µl of a dilution containing 0.1% Triton X-100 and the desired concentration of Cry1Ac to the surface of solidified Southland diet in each well of 128-well bioassay trays (C-D International, Pitman, NJ, USA). One neonate (< 8 h old) was transferred to each well and trays were covered with ventilated plastic lids (C-D International) and held for 7 days under the abiotic conditions mentioned above.

We conducted five sets of bioassays using GA-RS neonates from the F2 (July 2018), F12 (July 2019), F22 (June 2020), F23 (July 2020), and F26 (October 2020) generations (Supplementary Table S1). Neonates were exposed to diet with 0 (control), 1, or 10 µg Cry1Ac per cm^2 diet. After 7 days, live first instar larvae on diet with 1 µg Cry1Ac per cm^2 were considered susceptible because this low toxin concentration inhibited their growth, whereas live larvae on diet with 10 µg Cry1Ac per cm^2 that were third or subsequent instars were considered resistant

because they grew well despite this high toxin concentration. For control larvae reared on diet without Cry1Ac, mean survival to third instar was 96% (range: 91-100%, mean n = 99 larvae per bioassay in five bioassays). Susceptible, resistant, and control larvae were transferred individually to plastic cups containing non-Bt diet, reared to fifth instar, transferred individually to 1.5 ml plastic tubes, and frozen at -80°C for subsequent genomic comparison.

Genomic comparison of GA-R and LAB-S

We sequenced pools of larvae from the parental strains GA-R and LAB-S, which allowed us to evaluate genetic variation between and within these parental strains. This also allowed us to check if SNPs associated with resistance in the GWAS of GA-RS were more common in GA-R, and if those associated with susceptibility were more common in LAB-S. In April 2019, we collected 30 third instars from each strain, extracted DNA using Qiagen DNeasy Blood and Tissue Kits (Qiagen, Hilden, Germany), and constructed Illumina libraries using KAPA LTP Library Preparation Kits (Roche, Basel, Switzerland). We sequenced both libraries on an Illumina HiSeq4000 at Novogene (Beijing, China). We called variants with Platypus after read trimming and alignment to the genome using Trimmomatic and bwa-mem as described above. To detect potential selective sweeps in each strain, we used SAMtools mpileup (Li 2011) and PoPoolation (Kofler *et al.* 2011) to calculate Tajima's D in 50-kb windows overlapping by 10 kb across the genome.

Genome-wide association study for Cry1Ac resistance

From the heterogeneous strain GA-RS F12 larvae phenotyped in July 2019, we extracted DNA from 144 resistant and 144 susceptible larvae using ZYMO *Quick-DNA* 96 Plus Kits and quantified the DNA concentration of each individual using a Nanodrop (Thermo Fisher Scientific, Waltham, MA, USA). We combined equal amounts of DNA from each of the 144 resistant larvae to make a resistant pool and from each of the 144 susceptible larvae to make a susceptible pool, then generated libraries using KAPA LTP Library Preparation Kits for each

pool. We sequenced both libraries on an Illumina HiSeq4000 at Novogene (Beijing, China).

We demultiplexed reads and trimmed for adapter contamination and low-quality sequence using Trimmomatic (Bolger *et al.* 2014). We mapped reads to the *de novo H. zea* genome using bwa-mem (Li and Durbin 2009). We used Platypus (Rimmer *et al.* 2014) to call and quantify SNP variants and short INDELs. We extracted biallelic SNPs with a minimum coverage of 20 in each pool and a total coverage between 60 and 500 from the Platypus output for statistical analysis, for which we used two approaches (Benowitz *et al.* 2019). First, we calculated a Z-statistic (Huang *et al.* 2012), using the formula $Z = \frac{\rho_1 - \rho_2}{\sqrt{(\rho_0(1-\rho_0)(\frac{1}{n}+\frac{1}{c_1}+\frac{1}{c_2})}}$, where ρ_1 and ρ_2 are the reference alleles frequencies of each bulk, ρ_0 is the mean allele frequency across bulks, n is the sample size of each bulk, and c_1 and c_2 are the read depth of each bulk. We evaluated statistical significance of Z against the standard normal distribution. Following convention (Barsh *et al.* 2012, Welter *et al.* 2014), we used $P < 5 \times 10^{-8}$ as a threshold for significance. To estimate the density of significant sites, we used the R package WindowScanR (https://github.com/tavareshugo/WindowScanR) to calculate the percentage of SNPs with a more liberal threshold of $P < 10^{-5}$ in 10-kb windows overlapping by 5 kb. Density of significant sites may be a particularly useful parameter because the magnitude of each individual *P*-value from a bulk segregant analysis is highly sensitive to noise. Close linkage to the causal allele, however, should result in a higher density of significant sites even if the *P*-value itself varies. Second, we performed a sliding-window analysis with 500-kb windows overlapping by 250 kb using the R package QTLseqr (Mansfeld and Grumet 2018), which implements the G´ method of Magwene *et al.* (2011). This method provides a statistical determination of whether an entire QTL, rather than an individual SNP, is significant, and also defines borders to QTLs deemed significant.

Fine-scale mapping within chromosome 13

Using larvae from the F22 and F23 generation (July 2020), we conducted fine-scale mapping within the QTL in chromosome 13 associated with resistance, which we refer to hereafter as the *r1* locus. Using the methods described above, larvae were scored as resistant or susceptible.

After phenotyping, we reared susceptible larvae to fifth instars on untreated diet before storing all larvae (62 resistant and 51 susceptible) at -80°C. We extracted DNA from each sample using Qiagen DNeasy Blood and Tissue Kits and genotyped each larva individually via high-resolution melt curve (HRM) analysis at 12 SNP marker sites within the chromosome 13 QTL (Supplementary Table S2). For each site, we performed PCR in 10 µl reactions using Apex Taq DNA polymerase and EvaGreen Dye (Biotium, Fremont, CA, USA) as the intercalating dye. We ran RT-PCR in a QuantStudio 3 Real-Time PCR machine (Thermo Fisher) using continuous capture with a 0.025°C/s ramp. We used QuantStudio Design and Analysis Software (Thermo Fisher) to manually score melt curves for the identity of the focal SNP. We compared test melt curves against control curves generated from the parental LAB-S and GA-R strains. We used Fisher's exact test to assess significant differences between allele frequencies of resistant and susceptible individuals.

The lack of amplification from some individuals for some markers yielded variation in sample size among the 12 markers. These ranged from 40 to 60 for resistant larvae (mean = 56) and 20 to 50 (mean = 45) for susceptible larvae. We also used HRM to obtain genotypes at marker #4 for 23 of 25 resistant larvae and 89 of 95 control larvae tested from the F26 generation. The control larvae were not screened with a bioassay and thus contained a mixture of resistant and susceptible individuals.

To confirm the accuracy of HRM genotyping, we Sanger sequenced a single site (marker 4; Supplementary Table S2) for all 60 resistant and a subset of 34 susceptible individuals. We designed new primers to produce a longer amplicon, and confirmed the quality of the resultant amplicons with gel electrophoresis. We cleaned the PCR product with Exonuclease I and Antarctic Phosphatase (New England BioLabs, Ipswich, MA, USA) before sending to Eurofins Genomics (Louisville, KY, USA) for Sanger sequencing.

In addition to the fine mapping data from the HRM, we used the data on significant SNP density from the original GWAS experiment as well as the Tajima's D results from comparison of the GA-R and LAB-S strains to provide additional support for narrowing the region associated with resistance within chromosome 13.

296

297 **Inheritance and trajectory of resistance in GA-RS**

298 We performed several analyses of genotype frequencies at marker 4 to understand how *r1* affects
299 resistance. We used the genotypes from the RNA-seq study (see below) as a control group to
300 examine the frequency of marker 4 in the GA-RS strain at the F26 generation. We also used a χ^2
301 test to examine departure from Hardy-Weinberg equilibrium.

302 We used Fisher's exact test to determine if resistant individuals from GA-RS were more likely to
303 be homozygous for alleles from GA-R (GG) than heterozygous with one allele from GA-R and
304 the other from LAB-S (GL) by comparing the frequencies of each genotype in the resistant
305 samples from generations F22, F23, and F26 to the control samples from generation F26. We
306 calculated the dominance parameter *h*, which varies from 0 for recessively inherited resistance to
307 1 for dominantly inherited resistance (Liu and Tabashnik 1997), using the genotype frequencies
308 at marker 4 in the F22, F23, and F26 for resistant, control, and susceptible larvae (Supplementary
309 Table S3). The results from F22 and F23 were similar and were pooled to increase the sample
310 size for analyses.

311 To evaluate the relationship between genotype and resistance, we compared their trajectories
312 across generations in GA-RS. We used linear regressions in R 4.1.0 to test the null hypothesis of
313 no change in the $\log_{10}$ of percentage survival to third instar. Bioassays used 1 or 10 µg of Cry1Ac
314 per cm^2 in generations F2, F22 and F23, and only the higher concentration in the F26 test.

315

316 **RNA-seq and candidate gene analysis**

317 To generate samples for RNA sequencing, we reared LAB-S, GA-R, and GA-RS (generation 26)
318 individuals on untreated diet as described above in October 2020. When the larvae of the
319 parental strains LAB-S and GA-R reached the third instar, we dissected midguts from 15
320 individuals and froze them in groups of five, generating three biological replicates per strain. For
321 the GA-RS heterogeneous strain, we dissected 95 third instar midguts and froze them

individually, while simultaneously freezing the remainder of the carcass separately in wells of a PCR plate. We extracted DNA from each sample using a squish extraction (Gloor *et al.* 1993) using 50 µl of buffer. We screened samples HRM as above at marker 4, which was one of two sites we found to be most strongly associated with resistance. We selected 15 individuals that were homozygous for the LAB-S genotype at this site (henceforth "LL") and 15 individuals homozygous for the GA-R genotype at this site (henceforth "GG") and pooled the midguts corresponding to these samples into groups of five, again generating three biological replicates for each genotype. Selecting genotypes in this way allowed us to isolate the effects that the chromosome 13 QTL has on gene expression, giving us the potential to detect *trans*-regulatory effects. We extracted RNA from all 12 midgut samples using ZYMO Direct-zol RNA Miniprep Kit kits and built paired-end libraries with KAPA stranded mRNA seq kits. Libraries were sequenced in part on an Illumina NextSeq at the University of Arizona Genetics Core (UAGC; Tucson, AZ, USA) and part on an Illumina NovaSeq at Novogene.

We trimmed reads using Trimmomatic (Bolger *et al.* 2014) and aligned them to our *H. zea* assembly with Hisat2 (Kim *et al.* 2019). We built genome-guided transcriptome assemblies for each sample using StringTie (Pertea *et al.* 2016) and used StringTie merge to create a single transcriptome. We used blastp to identify the closest ortholog in *H. armigera* for each gene. We quantified read abundance for each sample using Salmon (Patro *et al.* 2017) and combined its transcript-level counts into gene-level counts with the R package tximport (Soneson *et al.* 2016). We analyzed differential expression using FDR-corrected *P*-values from negative binomial models at the gene level with edgeR (Robinson *et al.* 2010), after filtering and normalization for library-size differences. We performed statistical comparisons of LAB-S to GA-R and LL to GG. We performed a one-tailed (to account for directionality of gene expression differences) χ^2 test to examine whether the overlap of differentially expressed (DE) genes was more than expected by chance.

In addition to analyzing global differential expression, we used the RNA-seq data to better understand gene structure and expression within the candidate QTL. For each sample, we used Trinity (Haas *et al.* 2013) to construct *de novo* transcriptome assemblies for each sample. Using tblastn, we identified the transcripts in each Trinity assembly corresponding to all StringTie transcripts from the region from bp 4,370,000 – 4,620,000. We then took the longest transcript

from each Trinity assembly and used orfipy (Singh and Wurtele 2021) to extract the longest open reading frame (ORF) for each gene. Next we compared the ORFs from each of the 12 samples, looking for differences in predicted protein structure between the samples with resistant chromosome 13 genotypes (GA-R and GG) and susceptible ones (LAB-S and LL). We quantified midgut abundance of transcripts for all genes expressed in this region with average log count per million reads across all samples produced by edgeR. We used PROVEAN (Choi and Chan 2015) to predict the effects of amino acid substitutions between LAB-S and GA-R for each of the genes in this region.

After identifying a nonsense mutation in the *kinesin-12* gene, we manually inspected this site in IGV (Robinson *et al.* 2017). After performing Sanger sequencing of the GA strain and field samples (see below), we additionally inspected this site by visualizing sequencing chromatograms in Teal (Rausch *et al.* 2020). We analyzed the putative kinesin-12 protein computationally using blastp to find homologous proteins. We then used blastp to compare the sequence conservation upstream and downstream of the stop codon mutation in the lepidopteran species *H. armigera* (XP_021193241.1), *Chloridea virescens* (PCG76683.1), *Spodoptera litura* (XP_022828947.1), *Manduca sexta* (KAG6448083.1), and *Bombyx mori* (XP_004927959). We used a two-tailed paired t-test to assess amino acid conservation across these species before and after the nonsense mutation. We aligned these sequences with both the GA-R and LAB-S *H. zea* sequences with Clustal Omega (Sievers and Higgins 2018) and plotted the alignments using TeXshade (Beitz 2000). To further probe the potential structure and function of the protein, we used InterProScan 5 (Jones *et al.* 2014) to search for additional protein domains, AlphaFold 2.1.0 (Jumper *et al*. 2021) to predict the 3D protein structure, SignalP 5.0 (Armenteros *et al.* 2019) to examine if the protein contained signal peptides, and DeepGOPlus (Kulmanov and Hoehndorf 2020) to predict gene ontology (GO; Ashburner *et al.* 2000) categorization based on the sequence.

Genotyping of the GA strain and field samples for the *kinesin-12* mutation

We collected *H. zea* larvae from the field in Maricopa, Arizona in October 2020 and Tifton,

Georgia in July 2021. Both populations had high resistance to Cry1Ac (Yu *et al.* 2021; Y. Carrière, unpubl. data). We reared larvae to adults in the lab and collected tissue from 25 of the Maricopa samples and 39 of the Tifton samples. We extracted DNA using a squish extraction (Gloor *et al.* 1993) in 150 µl of buffer. We analyzed five F72 GA individuals sequenced in October 2016 (Fritz *et al.* 2020). We downloaded raw reads from NCBI (PRJNA599999), trimmed them using Trimmomatic, aligned them to the GA-R genome with bwa-mem, and identified the frequency of the C546T mutation with samtools and VarScan. We additionally collected tissue from 20 F87 adults from the GA strain in May 2018 and extracted DNA with Qiagen DNeasy Blood and Tissue Kits. We designed primers (Supplementary Table S2) to amplify the region surrounding the *kinesin-12* mutation causing a stop codon. We performed PCR as above, although with the addition of final concentration 0.1 µg/µl bovine serum albumin (Sigma-Aldrich, St. Louis, MO, USA) due to PCR inhibitors. Sanger sequencing was done at Eurofins Genomics as described above. We screened sequences manually in Geneious Prime (Biomatters, Auckland, NZ) for presence of the target mutation.

Analysis of 11 genes previously implicated in lepidopteran resistance to Cry1Ac

We used our results from GWAS and RNA-seq to test the hypothesis that one or more of 11 genes previously implicated in lepidopteran resistance to Cry1Ac contributed to resistance in our strains. For each gene, we present the lowest *P*-value from the original GWAS of SNPs between the start and end of the gene in the G´ analysis. We also report the FDR corrected *P*-values from differential expression analyses in edgeR comparing GA-R versus LAB-S and within GA-RS comparing individuals with both alleles from GA-R (GG) versus those with both alleles from LAB-S (LL).

Results

Chromosome-level assembly of the genome of resistant strain GA-R of *H. zea*

We generated a *de novo* chromosome-level assembly of the genome of the GA-R strain of *H. zea* with 31 chromosomes, 375.2 Mb, 36.9% GC content, 33.0% repeat content, an N50 scaffold length of 12.9 Mb, and 15,482 encoded proteins (Supplementary Table S4). Of 5,286 conserved single-copy lepidopteran genes, this genome has 98.9% complete, 98.5% complete and single-copy, 0.4% duplicated, 0.3% fragmented, and only 0.8% missing. The new genome assembly has only one gap set to 100 bp, which occurs in chromosome 17 and represents 0.000027% of the genome. This is a considerable improvement from the *H. zea* assembly of Pearce *et al.* (2017), which has 34.1 Mb of gaps representing 10% of that genome (Supplementary Table S4). Relative to the previous *H. zea* genome assembly, the new assembly has 64-fold greater N50, 10% more base pairs, 15% more complete BUSCO genes, and double the repeat content (Supplementary Table S4). Relative to previous estimates based on bacterial artificial chromosome sequencing and flow cytometry, the new genome size is 3% larger than an estimate for *H. zea* (Coates *et al.* 2017) and 5% smaller than an estimate for *H. armigera* (Zhang *et al.* 2019b).

The 31 chromosomes in the new assembly are largely syntenic with those of *H. armigera* (Pearce *et al.* 2017; Valencia-Montoya *et al.* 2020), although with different inversion karyotypes for 19 chromosomes (Supplementary Figure S1). We also found substantial differences between *H. zea* and *H. armigera* in the Z chromosome (chromosome 1) that are not associated with reversed sequences and thus probably not caused by chromosomal inversions (Supplementary Figure S1). An alternative hypothesis is that errors in one or both assemblies contributed to these differences. Errors are less likely in the new *H. zea* assembly because of its higher N50 and lower gap percentage relative to the *H. armigera* assembly (Supplementary Table S4, Pearce *et al.* 2017). In particular, the Z chromosome assembled cleanly without additional merging in the new *H. zea* assembly.

Genomic comparison between GA-R and the susceptible strain LAB-S

Sequencing of 30 larvae from GA-R and 30 larvae from the unrelated susceptible strain LAB-S revealed 165,416 fixed differences between the strains, as well 941,146 variable sites in GA-R and 911,946 in LAB-S. Analysis of Tajima's D showed many regions with low genetic variation throughout the genome in both strains (Supplementary Figures S2 and S3). For both strains,

these regions could reflect genetic drift or selective sweeps caused by adaptation to lab conditions. For GA-R, regions of low variation could also reflect selection for resistance in the lab.

Genome-Wide Association Study (GWAS) of resistance to Cry1Ac in GA-RS

We created the GA-RS strain by crossing GA-R and LAB-S. Both the Z-score and G´ sliding window analyses of 1,578,733 SNPs from the GWAS using pools of resistant and susceptible larvae from the F12 generation of GA-RS identified a region associated with resistance on chromosome 13 (Figure 1, Supplementary Figure S4). G´ analysis via QTLseqr defined this QTL as a region from 4.0 to 6.5 Mb. This QTL contains 117 SNPs associated with resistance at $P < 5 \times 10^{-8}$. All of these 117 SNPs showed the expected relationship with the parental strain. The 108 alleles found at higher frequency in the resistant larvae were more common in GA-R than LAB-S. The remaining nine alleles were at higher frequency in the susceptible larvae and were more common in LAB-S than GA-R.

Outside of this QTL, only 18 SNPs were associated with resistance at $P < 5 \times 10^{-8}$. Both chromosome 10 and 15 had two of these SNPs. No other chromosome had more than one. In the G´ analysis, only the QTL on chromosome 13 was significantly associated with resistance (Supplementary Figure S4). We refer to this QTL as the *r1* locus.

Analysis of Z-scores from the GWAS shows that SNP sites that differed significantly between resistant and susceptible larvae were not evenly distributed across the chromosome 13 QTL (Figure 2A). Eighteen of the 25 windows of 10 kb with the top 5% significant SNP density were clustered between 4.42 and 4.60 Mb. Consistent with the GWAS results, Tajima's D provides evidence for a selective sweep in GA-R between 4.3 and 5.2 Mb on chromosome 13 (Figure 2B).

Fine-scale mapping within the *r1* locus

We used HRM to genotype individual resistant and susceptible larvae from the F22 and F23 of

GA-RS for SNPs at 12 marker sites within *r1*. This revealed eight markers (2 to 9) from 4.3 to 5.0 Mb significantly associated with resistance (Table 1). For marker 4 at 4.5 Mb (n = 57) and marker 5 at 4.6 Mb (n = 60), all resistant larvae genotyped from GA-RS were either homozygous for the allele from the resistant GA-R strain (GG) or heterozygous, with one allele from GA-R and the other from the susceptible LAB-S strain (GL) (Table 1). These results were confirmed via Sanger sequencing for all 60 resistant individuals and 34 susceptible individuals. A similar test using only resistant larvae from the F26 confirmed this result: all 23 resistant larvae genotyped were either GG (16) or GL (7). By contrast, the three genotypes were in Hardy-Weinberg equilibrium in 89 larvae genotyped from a control sample from the F26 that was not screened for resistance and thus contained a mixture of resistant and susceptible individuals (24 GG: 44 GL: 21 LL, $\chi^2 = 0.0091$; $P = 0.52$). Genotype frequency in the F26 larvae differed significantly between the resistant larvae and the control larvae ($\chi^2 = 22.60$, $P = 1.2 \times 10^{-5}$).

The results from the GWAS, Tajima's D, the G´ analysis, analysis of SNP density, and fine-scale mapping (Figures 1 and 2, Table 2), identify the region between 4.3 to 4.6 Mb as most likely to contain the mutation(s) causing the effect of chromosome 13 on resistance to Cry1Ac. This region is captured by a single contig in both our Canu and DBG2OLC assemblies (Supplementary Figure S5) and is syntenic with a region of the *H. armigera* chromosome 13 (Supplementary Figures S1 and S6).

Gene expression in the midgut and a stop codon in *r1*

Based on the results above and annotations from funannotate and StringTie, we focused on the 10 genes between 4.37 and 4.62 Mb on chromosome 13. Six of these 10 genes were expressed substantially in the midgut of third instar larvae (Figure 3A, Table 2). The most highly expressed gene encodes a wild-type protein of 308 amino acids that has sequence identity of 97% with *kinesin-related protein 12* in *H. armigera* (XP_021193241; Supplementary Figure S7, Supplementary Table S5). The structure of this gene in terms of introns and exons is also similar between *H. zea* and *H. armigera* (Supplementary Figure S6B). Hereafter, we refer to this gene in *H. zea* as *kinesin-12*.

In GA-R we found a point mutation (C546T) in *kinesin-12* that introduces a premature stop codon expected to truncate the protein at 183 amino acids (Figure 3B, Supplementary Figure S7). Manual inspection of aligned genomic reads, RNA-seq reads, and Sanger sequences further confirmed the identity of the SNP (Supplementary Figures S7, S8 and S9). This mutation occurred in 100% of reads covering the SNP from 30 GA-R larvae and in 0% of reads covering the SNP from 30 LAB-S larvae that were sequenced in the genomic comparison between these strains. In the GWAS with GA-RS, this mutation was more common in resistant larvae (71%) than susceptible larvae (32%; $P = 7.48 \times 10^{-6}$). It occurs at bp 4,547,246, between the two markers (4 and 5) most tightly associated with resistance to Cry1Ac (Table 1). Furthermore, RNA-seq near marker 4 detected the C546T mutation in 100% of reads covering the SNP from 15 GG larvae and 0% of reads covering the SNP from 15 LL larvae, confirming complete linkage between this mutation and marker 4. All of this evidence identifies the C546T mutation in *kinesin-12* as a candidate for causing the contribution of the *r1* allele to resistance to Cry1Ac.

Aside from the *kinesin-12* mutation, we detected missense mutations between GA-R and LAB-S linked to marker 4 in three of the other six candidate genes in this region that were expressed substantially in midguts of third instar larvae. These genes encode juvenile hormone esterase, phosphatidylinositol 4-phosphate 3-kinase, and ubiquitin protein ligase (Table 2). However, according to PROVEAN, none of the amino acid substitutions in these genes are expected to have major effects on protein function.

Although the *kinesin-12* gene has been annotated as encoding a kinesin-related protein in *H. armigera*, both its wild-type function and the effects of the nonsense mutation remain unclear. Within the moth family Noctuidae, amino acid sequence identities relative to the LAB-S strain of *H. zea* are 97% for *H. armigera* (as noted above), 87% for *C. virescens*, and 61% for *S. litura* (Supplementary Table S5). Outside this family, no annotated proteins in Lepidoptera have greater than 45% amino acid identity and we found no orthologs in other insect orders. For five species of Lepidoptera, including the three mentioned above plus *B. mori* and *M. sexta*, the sequence identity for this protein relative to LAB-S did not differ significantly between upstream and downstream from the stop codon ($t_4 = 0.95$, $P = 0.40$; Supplementary Table S5). Thus, we cannot reject the null hypothesis that evolutionary constraints are similar for the portions of the protein before and after the stop codon.

519 Analysis with SignalP found no evidence for a signal peptide, indicating this protein is not likely
520 to be integrated into or secreted through the cell membrane. The most specific of the GO terms
521 associated with this protein by DeepGoPlus (Supplementary Table S6) is intracellular non-
522 membrane-bounded organelle, which is most closely associated with kinesin-related proteins in
523 *Drosophila melanogaster* (http://amigo.geneontology.org/amigo/term/GO:0043232).
524 InterProScan and AlphaFold identified a coil with high confidence (aa 124-194; Supplementary
525 Figures S11 and S12) that would be disrupted in the truncated form of the protein. Thus, we find
526 moderate evidence the *H. zea kinesin-12* gene encodes a kinesin protein whose function might be
527 disrupted by the C546T nonsense mutation.

528

529 **_Kinesin-12_ mutation in the GA strain and in field samples**

530 To test the hypothesis that the C546T mutation in *kinesin-12* originated in the field, we
531 determined its frequency in the GA strain of *H. zea*, which was selected for resistance in the
532 field, but not in the lab (Brévault *et al.* 2013; Welch *et al.* 2015). In GA, the frequency of the
533 C546T mutation was 0.80 in five larvae from the F72 generation (three with homozygous TT
534 genotypes and two with heterozygous CT genotypes), which does not differ significantly from its
535 frequency of 0.975 in 20 larvae from the F87 generation (19 homozygous TT and one
536 heterozygous CT; Fisher's exact test: $P = 0.10$). These results are consistent with the hypothesis
537 that C546T mutation originated in the field population from which GA was established. The
538 alternative hypothesis that this mutation was absent in the field and arose in the lab seems
539 unlikely. Based on the mean of ca. 900 moths per generation for GA and assuming a mutation
540 rate of 3×10^{-9} per nucleotide site (Keightley *et al.* 2015; Yoder and Tiley 2021), the probability
541 of a single mutation arising at a particular nucleotide site in GA during 72 generations is 0.0004.

542 The high frequency of C546T in GA after rearing for many generations in the lab without
543 exposure to Bt toxins implies this mutation caused little or no fitness cost when reared in the lab
544 in the absence of Bt toxins. However, we did not find this mutation in 39 individuals collected
545 from the field in Georgia in July 2021 or in 25 individuals derived from the field in Arizona in
546 2020, despite the resistance to Cry1Ac in both of these field populations (Yu *et al.* 2021; Y.

Carrière, unpubl. data). Whereas all individuals from the Georgia 2021 sample had the same sequence as LAB-S at the codon starting with bp 546, three individuals from Arizona had a single base pair substitution (C546A) changing the encoded amino acid from glutamine to lysine. In the field samples from Arizona in 2020 and Georgia in 2021, we detected no insertions, deletions, or other mutations introducing a stop codon in the 200 bp upstream or downstream from the C546T mutation.

Inheritance and trajectory of resistance in GA-RS

The genotype frequencies at marker 4 in resistant and susceptible larvae indicate at least one GA-R allele at this locus was necessary for resistance in our screening bioassay at 10 µg Cry1Ac per cm^2 diet (Table 1). However, 27% of susceptible larvae were homozygous for the GA-R allele at marker 4 (Table 1). Together these results suggest that the *r1* allele was necessary but not sufficient for resistance to Cry1Ac in our screening bioassay.

Compared to 89 control larvae reared on untreated diet, 69 resistant larvae from the F22, F23, and F26 generations had a significantly higher ratio of the GG genotype to the GL genotype for marker 4 (Fisher's exact test; $P < 0.0001$). Based on the data for marker 4 from the F22, F23, and F26, the *r1* allele had a value for dominance (h) of 0.23 (Supplementary Table S3), which is intermediate between completely recessive inheritance ($h = 0$) and additive inheritance ($h = 0.5$).

To test the hypothesis that alleles at one or more other loci contributed to resistance, we compared the trajectory of resistance based on bioassay data with the trajectory of the GA-R allele at marker 4. Resistance to Cry1Ac decreased substantially over time (Figure 4; Supplementary Table S1), indicating that in the absence of Cry1Ac, a pleiotropic fitness cost was associated with one or more alleles contributing to resistance. However, the frequency of the GA-R allele at marker 4 was 0.52 in 89 control larvae from the F26, which is not different than the expected 0.50 in the F1. This suggests no fitness cost was associated with the *r1* allele, which is tightly linked with GA-R allele at marker 4. In the F26, marker 4 was in Hardy-Weinberg equilibrium as noted above, confirming the absence of selection at this locus in GA-RS. The significant decrease in resistance over time despite no decline in the frequency of the GA-R

575 allele at marker 4 implies the decrease in resistance was caused by reduced frequency of one or
576 more resistance alleles that carry a fitness cost in the absence of Cry1Ac and are not linked with
577 the *r1* allele.

578

579 **Analysis of gene expression using RNA-seq**

580 To test the hypothesis that differential gene expression contributes to resistance, we used RNA-
581 seq to compare transcript levels between GA-R and LAB-S and between the GG and LL
582 genotypes within GA-RS. After filtering, we analyzed expression of 12,965 genes
583 (Supplementary Table S7). We found 2,173 differentially expressed (DE) genes between the
584 unrelated strains LAB-S and GA-R (Supplementary Table S8) and 23 DE genes between the GG
585 and LL genotypes within GA-RS (Supplementary Table S9). None of the genes associated with
586 *r1* in chromosome 13 differed significantly in expression between GA-R and LAB-S or between
587 GG and LL.

588 Twelve of the 23 DE genes between GG and LL were also among the set of 2,173 DE genes in
589 the parental strain comparison, of which nine were DE in the same direction in both comparisons
590 (higher expression in GA-R than LAB-S and in GG than LL or vice versa; Tables S6 and S7).
591 The overlap in DE genes between these two datasets is significantly greater than expected by
592 chance ($\chi^2 = 3.86$; $P = 0.025$), implying the within-strain comparison between GG and LL
593 reflects meaningful differences between the parental strains. However, none of the 23 DE genes
594 between GG and LL (Supplementary Table S9) are among the 11 genes previously implicated in
595 resistance to Cry1Ac in lepidopterans (Table 3). One gene significantly downregulated in both
596 GA-R and GG is on chromosome 1 and encodes a sodium/potassium/calcium
597 exchanger (Supplementary Tables S8 and S9). This transmembrane protein has some functional
598 similarities to ABC transporters and could be a candidate as a Bt receptor. However, expression
599 was reduced only 2.6-fold in GG versus LL and 2.5-fold in GA-R versus LAB-S. Together these
600 results indicate the *r1* region exerts a *trans*-regulatory effect on gene expression, but the current
601 data provide no compelling evidence that any difference in expression influences resistance.

602

Analysis of 11 genes previously implicated in lepidopteran resistance to Cry1Ac

We used our results from GWAS and RNA-seq to evaluate potential contributions to resistance of 11 genes previously implicated in lepidopteran resistance to Cry1Ac (Table 3). None of these candidate genes are in the resistance-associated QTL on chromosome 13 or the putative minor effect QTL on chromosome 10 (Table 3). In addition, none of them had any SNPs that were significantly associated with resistance in the GWAS (Table 3). Although *tetraspanin-1* is on chromosome 10 in *H. zea*, it is outside the regions of this chromosome that were moderately associated with resistance in the GWAS. As noted above, none of the 23 DE genes between GG and LL are among the 11 candidate genes (Supplementary Table S9). Only one of the 11 pairwise comparisons between strains based on RNA-seq showed a significant difference. Expression of *ABCC1* was significantly lower in GA-R than LAB-S ($P = 0.0014$, Table 3; Table S6). However, within GA-RS, expression of *ABCC1* did not differ significantly between GG and LL ($P = 0.29$; Table 3), which indicates reduced expression of *ABCC1* was not genetically linked with resistance conferred by *r1*.

Discussion

We report three key results demonstrating a novel genetic basis of Cry1Ac resistance in the GA-R strain of *H. zea*, which resulted from field selection followed by lab selection (Brévault *et al.* 2013; Welch *et al.* 2015). First, resistance was associated with a 250-kb region of chromosome 13 that contains no genes with a previously identified role in Bt resistance or toxicity. Second, within this region, resistance to Cry1Ac was associated with a point mutation that introduces a premature stop codon in a novel candidate gene, *kinesin-12*. Third, we report evidence that one or more other loci also contributed to resistance to Cry1Ac. To facilitate these advances, we built the first chromosome-level genome assembly for *H. zea*, adding to a growing set of highly contiguous genomes for lepidopteran pests (Chen *et al.* 2019b; Ward *et al.* 2021; Yan *et al.* 2021). This genome was essential for the genetic mapping reported here and will serve as a resource for other genomic investigations into the biology of *H. zea*.

Our findings add a new candidate gene to the diverse list of genes associated with Bt resistance

in lepidopterans (Jin *et al.* 2018; Guo *et al.* 2021; Jurat-Fuentes *et al.* 2021). However, the novel genetic basis of resistance does not necessarily imply a novel biochemical mechanism of resistance. The effects of *r1* could be mediated by either decreased toxin activation or reduced binding of Cry1Ac to larval midgut membranes, which are well known mechanisms of Bt resistance (Peterson *et al.* 2017; Jurat-Fuentes *et al.* 2021). Indeed, previous studies of *H. zea* have found decreased protoxin activation in GA-R (Zhang *et al.* 2019) and reduced binding of Cry1Ac to larval midgut preparations in strains with resistance caused by knocking out the putative receptor ABCC2 (Perera *et al.* 2021).

The location of *r1* on chromosome 13 is noteworthy because it corresponds closely to the region under the strongest selection in *H. zea* populations from Louisiana that were exposed to Bt crops over the past 19 years (Taylor *et al.* 2021). Although Taylor *et al.* (2021) identified a narrow region near but not containing *r1* as the most likely site of selection (~4.0 Mb in our assembly), the broader region associated with the selective sweep in their data includes *r1* (~3.8 to 5.8 Mb) and aligns with both our original and refined QTL for resistance. Thus, *r1* might be associated with resistance to Cry1Ab (which is similar to Cry1Ac) in the field populations of *H. zea* from Louisiana studied by Taylor *et al.* (2021), as well as in GA-R and its parent strain GA (Fritz *et al.* 2020), which originated from a field-selected population in Georgia in 2008 (Brévault *et al.* 2013).

The RNA-seq evidence does not support the hypothesis that altered transcription in the *r1* region causes resistance. Thus, a protein-coding mutation is more likely to be responsible for the contribution of the *r1* region to resistance. We hypothesize that this contribution is mediated by the premature stop codon in the *kinesin-12* gene. Among the protein-coding mutations in the candidate region, only this nonsense mutation that shortens the predicted protein by 40% is expected to have a major effect on protein function. Furthermore, of the 10 genes in the region tightly associated with resistance, midgut expression was highest for *kinesin-12*, suggesting a midgut function for the protein it encodes. Protein functional prediction algorithms including DeepGoPlus provide moderate support for the original annotation as a kinesin with a function in intracellular transport or structure. Nonetheless, we do not know the normal function of the kinesin-12 protein and cannot infer that the C546T mutation causes resistance. In future work, we aim to test the hypothesis that the C546T mutation contributes to resistance by determining if

resistance is reduced when we use CRISPR/Cas9 to replace the mutant sequence in GA-R with the wild type sequence from LAB-S (Jin *et al.* 2018; Fabrick *et al.* 2021). If disruption of the *kinesin-12* gene is not sufficient for resistance, as the results here imply, we expect that knocking out this gene would not cause resistance in a susceptible strain.

Kinesins and kinesin-related proteins are motor proteins important in microtubule function, chromosomal movement, and organelle transport (Ali and Wang 2020) that have not been associated previously with Bt resistance. Several kinesins are involved in mitogen-activated protein kinase (MAPK) signaling cascades (Liang and Yang 2019) and MAPK signaling is implicated in Bt resistance (Guo *et al.* 2015, 2020, 2021; Qin *et al.* 2021). Furthermore, a case of xenobiotic resistance in mice involved a mutant kinesin acting downstream of a MAPK (Watters *et al.* 2001). Thus, one hypothesis is that *kinesin-12* acts downstream of MAPK as part of the signaling cascade initiated when Cry1Ac binds to a midgut receptor. However, MAPK influences Bt resistance via downregulation of Bt receptors (Guo *et al.* 2015, 2020, 2021; Qin *et al.* 2021). Here we see no evidence for reduced transcription of putative receptors, making this an unlikely explanation for the link between *kinesin-12* and resistance.

Kinesins also play a role in the localization of transmembrane proteins to the cell membrane (Jana *et al.* 2021) and in intracellular cadherin trafficking (Phang *et al.* 2014). The transport functions of kinesins and kinesin-related proteins entail motor complexes of three or more proteins (Phang *et al.* 2014), suggesting interactions between different proteins could be interrupted to interfere with receptor transport to the membrane. We hypothesize that in the GA-R strain of *H. zea,* a truncated *kinesin-12* in combination with mutations affecting one or more of its interacting partners blocks proper localization of a Bt receptor on the membrane.

The results from GWAS and fine-scale mapping show the *r1* allele was necessary, but not sufficient for resistance in our screening bioassay, implying contributions from one or more additional loci. If a second unlinked mutation were also necessary for resistance in our screening bioassay, this would be expected to yield a second major peak in the GWAS, similar to the peak for the QTL in chromosome 13. The lack of a second major peak suggests that mutations in two or more unlinked loci could each cause resistance in combination with *r1* (e.g., *r1* plus mutation *X* or *r1* plus mutation *Y* could cause resistance).

690 The decline in resistance over time in GA-RS also implies more than one locus contributed to
691 resistance. While resistance to Cry1Ac declined significantly across generations in GA-RS, the
692 frequency of C546T and other *r1* linked alleles did not. After 22, 23 and 26 generations without
693 exposure to Bt toxins, it was not lower than its expected initial frequency of 0.50. Thus, the
694 decline in resistance reflects a decreased resistance allele frequency at one or more other loci.
695 Unlike the C546T mutation, which did not have a substantial fitness cost in the lab, the observed
696 decline in resistance suggests that a fitness cost was associated with at least one mutation at
697 another locus that contributed to resistance in GA-RS. Polygenic resistance to Cry1Ac or
698 Cry1Ab also has been reported in strains of *H. zea* unrelated to GA-R (Caccia *et al.* 2012;
699 Lawrie *et al.* 2020; Perera *et al.* 2021; Taylor *et al.* 2021) and in other species of Lepidoptera
700 (Kaur and Dilwari 2010; Zhao *et al.* 2021; Ma *et al.* 2022).

701 The results summarized above have implications for understanding the trajectory of the C546T
702 mutation in the field. The high frequency of the C546T mutation in the field-selected GA strain
703 that was started with 180 field-collected larvae suggests this mutation was common in 2008 in
704 the moderately resistant field population in Georgia from which GA was derived (Brévault *et al.*
705 2013). In the absence of exposure to Cry1Ac, the frequency of this mutation did not increase
706 significantly in GA from the F72 to F87 or in GA-RS from the expected frequency in the F1 to
707 the observed frequency in the F26. Thus, because GA was not exposed to Cry1Ac in the lab, it is
708 unlikely the frequency of this mutation was low initially in GA and subsequently increased
709 because of strong selection. Nonetheless, we did not detect this mutation in Cry1Ac-resistant
710 populations from the same site in Georgia in 2021 or in Arizona in 2020. Thus, this mutation is
711 not associated with resistance to Cry1Ac in all field populations of *H. zea*. Also, its frequency
712 apparently decreased in the field in Georgia from 2008 to 2021. One hypothesis is that the
713 frequency of this mutation decreased in Georgia because it has a substantial fitness cost under
714 field conditions, such as reduced overwintering survival (Carrière *et al.* 2001), which would not
715 be evident in the lab. The C546T mutation could have been replaced by one or more mutations
716 that have lower fitness costs (Guillemaud *et al.* 1998), confer higher resistance to Cry1Ac, and/or
717 confer resistance without contributions from mutations at other loci. More research is needed to
718 determine the function of kinesin-12 and its role in resistance, as well as the genetic basis of
719 Cry1Ac resistance in current field populations of *H. zea.*

Data and code availability

All raw sequence data is available at NCBI (Bioproject: PRJNA767434). Phenotypic data, HRM and Sanger genotyping data, initial and final genome assemblies, genome annotations, and scripts for analyses and figures are all available via OSF. Supplementary materials are available at figshare.

Acknowledgments

Mention of trade names or commercial products in this article is solely for the purpose of providing specific information and does not imply recommendation or endorsement by the U.S. Department of Agriculture. USDA is an equal opportunity provider and employer. We thank Xinzhi Ni for sending *H. zea* from Georgia; Alex Yelich and Chandran Unnithan for help with insect rearing and dissections; Yidong Wu, David Heckel, Megan Fritz, Katherine Taylor, Fred Gould, and Juan Luis Jurat-Fuentes for their valuable comments on the manuscript; and Jon Galina-Mehlman, Jayson Talag, and Dave Kudrna for their assistance and advice regarding PacBio and Illumina sequencing.

Author contributions

J.F., Y.C., B.E.T., and L.M.M. conceived and designed the project. K.M.B., C.W.A., B.A.D., and X.L. performed experiments and collected the data. K.M.B., C.W.A., Y.C., and B.E.T. analyzed data. K.M.B. and B.E.T. wrote the manuscript with input from all authors.

Funding

This work was supported by grants from the USDA National Institute of Food and Agriculture (Agriculture and Food Research Initiative 2020-67013-31924 and Biotechnology Risk

745 Assessment Research Grants Program 2020-33522-32268), Corteva Agriscience, and the Cotton
746 Insect Resistance Management (IRM) Technical Subcommittee of the Agricultural
747 Biotechnology Stewardship Technical Committee (ABSTC).

748

749 Conflicts of interest

750 As noted above, support for this study was provided in part by Corteva Agriscience and the
751 Cotton IRM Technical Subcommittee of the ABSTC.

752

753

754 Literature cited

755 Ali MI, Luttrell RG, Young III SY. 2006. Susceptibilities of *Helicoverpa zea* and *Heliothis*
756 *virescens* (Lepidoptera: Noctuidae) populations to Cry1Ac insecticidal protein. J Econ
757 Entomol. 99:164-175.
758 Ali I, Yang W-C. 2020. The functions of kinesin and kinesin-related proteins in eukaryotes. Cell
759 Adh Migr. 14: 139-152.
760 Anilkumar KJ, Rodrigo-Simón A, Ferré J, Pusztai-Carey M, Sivasupramaniam S, *et al.* 2008.
761 Production and characterization of *Bacillus thuringiensis* Cry1Ac-resistant cotton
762 bollworm *Helicoverpa zea* (Boddie). Appl Environ Microbiol. 74:462–469.
763 Armenteros JJA, Tsirigos KD, Sønderby CK, Peterson TN, Winther O, *et al.* 2019. SignalP 5.0
764 improves signal peptide predictions using deep neural networks. Nat Biotech. 37:420-
765 423.
766 Ashburner M, Ball CA, Blake JA, Botstein D, Butler H, *et al.* 2000. GeneOntology: tool for the
767 unification of biology. Nat Genet. 25:25-29.
768 Barsh GS, Copenhaver GP, Gibson G, Williams SM. 2012. Guidelines for genome-wide
769 association studies. PLoS Genet. 8:e1002812.
770 Baxter SW, Badenes-Pérez FR, Morrison A, Vogel H, Crickmore N, *et al.* Parallel evolution of

Bacillus thuringiensis toxin resistance in Lepidoptera. Genetics. 189:675-679.

Beitz E. 2000. TeXshade: shading and labeling of multiple sequence alignments using LaTeX2e. Bioinformatics. 16:135-139.

Benowitz KM, Coleman JM, Matzkin LM. 2019. Assessing the architecture of *Drosophila mojavensis* locomotor evolution with bulk segregant analysis. G3 (Bethesda). 9:1767-1775.

Bolger AM, Lohse M, Usadel B. 2014. Trimmomatic: a flexible trimmer for Illumina sequence data. Bioinformatics. 30:2114-2120.

Bravo A, Likitvivatanavong S, Gill SS, Soberón M. 2011. *Bacillus thuringiensis*: a story of a successful bioinsecticide. Ins Biochem Mol Biol. 41:423-431.

Brévault T, Heuberger S, Zhang M, Ellers-Kirk C, Ni X, *et al.* 2013. Potential shortfall of pyramided transgenic cotton for insect resistance management. Proc Natl Acad Sci USA. 110:5806-5811.

Brévault T, Tabashnik BE, Carrière Y. 2015. A seed mixture increases dominance of resistance to Bt cotton in *Helicoverpa zea*. Sci Rep. 5:9807.

Caccia S, Moar WJ, Chandrashekhar J, Oppert C, Anilkumar KJ, *et al.* 2012. Association of Cry1Ac toxin resistance in *Helicoverpa zea* (Boddie) with increased alkaline phosphatase levels in the midgut lumen. Appl Env Microbiol. 78:5690-5698.

Calles-Torrez V, Knodel JJ, Boetel MA, French BW, Fuller BW, *et al.* 2019. Field-evolved resistance of northern and western corn rootworm (Coleoptera: Chrysomelidae) populations to corn hybrids expressing single and pyramided Cry3Bb1 and Cry34/35Ab1 Bt proteins in North Dakota. J Econ Entomol. 112:1875-1886.

Carrière Y, Ellers-Kirk C, Patin AL, Sims M, Meyer S, *et al.* 2001. Overwintering cost associated with resistance to transgenic cotton in the pink bollworm. J. Econ. Entomol. 94:935-941.

Carrière Y, Crickmore N, Tabashnik BE. 2015. Optimizing pyramided transgenic Bt crops for sustainable pest management. Nat Biotechnol. 33:161-168.

Carrière Y, Degain BA, Unnithan GC, Harpold VS, Heuberger S, Li X, *et al.* 2018. Effects of seasonal changes in cotton plants on the evolution of resistance to pyramided cotton producing the Bt toxins Cry1Ac and Cry1F in *Helicoverpa zea*. Pest Man Sci. 74:627-637.

802 Carrière Y, Degain B, Unnithan GC, Harpold VS, Li X, *et al.* 2019. Seasonal declines in Cry1Ac
803 and Cry2Ab concentration in maturing cotton favor faster evolution of resistance to
804 pyramided Bt cotton in Helicoverpa zea. J Econ Entomol. 112:2907–2914.
805 Carrière, Y, Brown Z, Aglasan S, Dutilleul P, Carroll M, *et al.* 2020a. Crop rotation mitigates
806 impacts of corn rootworm resistance to transgenic Bt corn. Proc Natl Acad Sci USA.
807 117:18385-18392.
808 Carrière Y, Degain BA, Harpold VS, Unnithan GC, Tabashnik BE. 2020b. Gene flow between
809 Bt and non-Bt plants in a seed mixture increases dominance of resistance to pyramided Bt
810 corn in *Helicoverpa zea* (Lepidoptera: Noctuidae). J Econ Entomol. 113:2041–2051.
811 Carrière Y, Degain BA, Tabashnik BE. 2021. Effects of gene flow between Bt and non-Bt plants
812 in a seed mixture of Cry1A.105 + Cry2Ab corn on performance of corn earworm in
813 Arizona. Pest Manag Sci. 77: 2106–2113
814 Chakraborty M, Baldwin-Brown JG, Long AD, Emerson JJ. 2016. Contiguous and accurate de
815 novo assembly of metazoan genomes with modest long read coverage. Nuc Ac Res. 44:
816 e147.
817 Chen L, Wei J, Liu C, Niu L, Zhang C, *et al.* 2019a. Effect of midgut specific binding protein
818 ABCC1 on Cry1Ac toxicity against *Helicoverpa armigera*. Sci Ag Sin. 52:3337-3345.
819 Chen W, Yang X, Tetreau G, Song X, Coutu C, *et al.* 2019b. A high-quality chromosome-level
820 genome assembly of a generalist herbivore, *Trichoplusia ni*. Mole Ecol Res. 19:485-496.
821 Chin CS, Alexander DH, Marks P, Klammer AA, Drake J, *et al.* 2013. Nonhybrid, finished
822 microbial genome assemblies from long-read SMRT sequencing data. Nat Methods.
823 10:563-569.
824 Choi Y, Chan AP. 2015. PROVEAN web server: a tool to predict the functional effect of amino
825 acid substitutions and indels. Bioinformatics. 31: 2745-2747.
826 Coates BS, Abel CA, Perera OP. 2017. Estimation of long terminal repeat element content in the
827 *Helicoverpa zea* genome from high-throughput sequencing of bacterial artificial
828 chromosome pools. Genome. 60:310-324.
829 Cook DR, Threet M. 2019. Cotton insect losses – 2019.
830 https://www.entomology.msstate.edu/resources/2019loss.php
831 Dively GP, Venugopal PD, Bean D, Whalen J, Holmstrom K, *et al.* 2018. Regional pest
832 suppression associated with widespread Bt maize adoption benefits vegetable growers.

833 Proc Natl Acad Sci USA. 115:3320–3325.
834 Fabrick JA, LeRoy DM, Mathew LG, Wu Y, Unnithan GC, *et al.* 2021. CRISPR-mediated
835 mutations in the ABC transporter gene ABCA2 confer pink bollworm resistance to Bt
836 toxin Cry2Ab. Sci Rep. 11:10377.
837 Ferguson KB, Kursch-Metz T, Verhulst EC, Pannebakker BA. 2020. Hybrid genome assembly
838 and evidence-based annotation of the gg parasitoid and biological control agent
839 *Trichogramma brassicae*. G3 (Bethesda). 10:3533-3540.
840 Flynn JM, Hubley R, Goubert C, Rosen J, Clark AG, *et al.* 2020. RepeatModeler2 for automated
841 genomic discovery of transposable element families. Proc Natl Acad Sci USA 117:9451-
842 9457.
843 Fritz ML, Nunziata SO, Guo R, Tabashnik BE, Carrière Y. 2020. Mutations in a novel cadherin
844 gene associated with Bt resistance in *Helicoverpa zea*. G3 (Bethesda). 10:1563-1574.
845 Gahan LJ, Gould F, Heckel DG. 2001. Identification of a gene associated with Bt resistance in
846 *Heliothis virescens*. Science 293:857-860.
847 Gloor GB, Preston CR, Johnson-Schlitz DM, Nassif NA, Phillis RW, *et al.* 1993. Type I
848 repressors of *P* element mobility. Genetics. 135:81-95.
849 Guillemaud T, Lenormand T, Bourguet D, Chevillon C, Pasteur N, *et al.* 1998. Evolution of
850 resistance in *Culex pipiens*: allele replacement and changing environment. Evolution.
851 52:443-453.
852 Guo Z, Kang S, Chen D, Wu Q, Wang S, *et al.* 2015. MAPK signaling pathway alters expression
853 of midgut ALP and ABCC genes and causes resistance to *Bacillus thuringiensis* Cry1Ac
854 toxin in diamondback moth. PLoS Genetics. 11:e1005124.
855 Guo Z, Kang S, Sun D, Gong L, Zhou J, *et al.* 2020. MAPK-dependent hormonal signaling
856 plasticity contributes to overcoming *Bacillus thuringiensis* toxin action in an insect host.
857 Nat Commun. 11:3003.
858 Guo Z, Kang S, Wu Q, Wang S, Crickmore N, *et al.* 2021. The regulation landscape of MAPK
859 signaling cascade for thwarting *Bacillus thuringiensis* infection in an insect host. PLoS
860 Path. 17:e1009917.
861 Haas BJ, Papanicolau A, Yassour M, Grabherr M, Blood PD, *et al.* 2013. *De novo* transcript
862 sequence reconstruction from RNA-seq using the Trinity platform for reference
863 generation and analysis. Nat Prot. 8:1494-1512.

Hartke J, Schell T, Jongepier E, Schmidt H, Sprenger PP, *et al.* 2019. Hybrid genome assembly of a neotropical mutualistic ant. Genom Biol Evol. 11:2306-2311.

Heckel DG, Gahan LJ, Baxter SW, Zhao J-Z, Shelton AM, *et al.* 2007. The diversity of Bt resistance genes in species of Lepidoptera. J Inv Biol. 95:192-197.

ISAAA. 2019. Global status of commercialized biotech/GM crops: 2019. ISAAA Brief No. 55. ISAA: Ithaca, NY.

Jaworski CC, Allan CW, Matzkin LM. 2020. Chromosome-level hybrid de novo genome assemblies as an attainable option for nonmodel insects. Mol Ecol Res. 20:1277-1293.

Jin L, Wei Y, Zhang L, Yang Y, Tabashnik BE, *et al.* 2013. Dominant resistance to Bt cotton and minor cross-resistance to Bt toxin in Cry2Ab in cotton bollworm from China. Evol Appl. 6:1222-1235.

Jin L, Wang F, Guan J, Zhang S, Yu S, Liu Y *et al.* 2018. Dominant point mutation in a tetraspanin gene associated with field-evolved resistance of cotton bollworm to transgenic Bt cotton. Proc Natl Acad Sci USA. 115:11760-11765.

Jones P, Binns D, Chang HY, Fraser M, Li W, *et al.* 2014. InterProScan 5: genome-scale protein function classification. Bioinformatics. 30:1236-1240.

Jumper J, Evans R, Pritzel A, Green T, Figurnov M, *et al.* 2021. Highly accurate protein structure prediction with AlphaFold. Nature. 596:583-589.

Jurat-Fuentes JL, Karumbaiah L, Jakka SRK, Ning C, Liu C, *et al.* 2011. Reduced levels of membrane-bound alkaline phosphatase are common to lepidopteran strains resistant to Cry toxins from *Bacillus thuringiensis*. PLoS One. 6:e17606.

Jurat-Fuentes JL, Heckel DG, Ferré J. 2021. Mechanisms of resistance to insecticidal proteins from *Bacillus thuringiensis*. Annu Rev Entomol. 66:121-140.

Kajitani R, Toshimoto K, Noguchi H, Toyoda A, Ogura Y, *et al.* 2014. Efficient *de novo* assembly of highly heterozygous genomes from whole-genome shotgun short reads. Genom Res. 24:1384-1395.

Karsch-Mizrachi I, Nakamura Y, Cochrane G. 2012. The International Nucleotide Sequence Database Collaboration. Nuc Ac Res. 40:D33-D37.

Kaur P, Dilwari VK. 2011. Inheritance of resistance to *Bacillus thuringiensis* Cry1Ac toxin in *Helicoverpa armigera* (Hübner) (Lepidoptera: Noctuidae) from India. Pest Man Sci. 67:1294-1302.

895 Kaur G, Guo J, Brown S, Head GP, Price PA, *et al.* 2019. Field-evolved resistance of
896 *Helicoverpa zea* (Boddie) to transgenic maze expressing pyramided Cry1A.105.Cry2Ab2
897 proteins in northeast Louisiana, the United States. J Inv Pathol. 163:11-20.
898 Keightley PD, Pinharanda A, Ness RW, Simpson F, Dasmahapatra KK *et al.* 2015. Estimation of
899 the spontaneous mutation rate in *Heliconius melpomene.* Mol Biol Evol. 32:239-243.
900 Kim D, Paggi JM, Park C, Bennett C, Salzberg SL. 2019. Graph-based genome alignment and
901 genotyping with HISAT2 and HISAT-genotype. Nat Biotech. 37:907-915.
902 Kofler R, Orozco-terWengel P, De Maio N, Pandey RV, Nolte V, *et al.* 2011. PoPoolation: a
903 toolbox for population genetic analysis of next generation sequencing data from pooled
904 individuals. PLoS One. 6:e15925.
905 Koren S, Walenz BP, Berlin K, Miller JR, Bergman NH, *et al.* 2017. Canu: scalable and accurate
906 long-read assembly via adaptive k-mer weighting and repeat separation. Genom Res.
907 27:722-736.
908 Kulmanov M, Hoehndorf R. 2020. DeepGOPlus: improved protein function prediction from
909 sequence. Bioinformatics. 36:422-429.
910 Langmead B, Salzberg S. 2012. Fast gapped-read alignment with Bowtie 2. Nat Methods. 9:357-
911 359.
912 Lawrie RD, Mitchell III RD, Deguenon JM, Ponnusamy L, Reisig D, *et al.* 2020. Multiple
913 known mechanisms and a possible role of an enhanced immune system in Bt-resistance
914 in a field population of the bollworm, *Helicoverpa zea*: differences in gene expression
915 with RNAseq. Int J Mol Sci. 21:6528.
916 Lawrie RD, Mitchell III RD, Deguenon JM, Ponnusamy L, Reisig D, *et al.* 2022.
917 Characterization of long non-coding RNAs in the bollworm, *Helicoverpa zea*, and their
918 possible role in Cry1Ac-resistance. Insects. 13:12.
919 Li H. 2011. A statistical framework for SNP calling, mutation discovery, association mapping
920 and population genetical parameter estimation from sequencing data. Bioinformatics.
921 27:2987-2993.
922 Li H, Durbin R. 2009. Fast and accurate short read alignment with Burrows-Wheeler transform.
923 Bioinformatics. 25:1754-1760.
924 Liang Y-J, Yang W-X. 2019. Kinesins in MAPK cascade: how kinesin motors are involved in
925 the MAPK pathway? Gene. 684:1-9.

926 Liu Y, Tabashnik BE. 1997. Inheritance of resistance to the *Bacillus thuringiensis* toxin Cry1C
927 in the diamondback moth. Appl Env Microbiol. 63:2218-2223.
928 Liu C, Xiao Y, Li X, Oppert B, Tabashnik BE, *et al.* 2014. *Cis*-mediated down-regulation of a
929 trypsin gene associated with Bt resistance in cotton bollworm. Sci Rep. 4:7219.
930 Luttrell RG, Wan L, Knighten K. 1999. Variation in susceptibility of Noctuid (Lepidoptera)
931 larvae attacking cotton and soybean to purified endotoxin proteins and commercial
932 formulations of *Bacillus thuringiensis*. J Econ Entomol. 92:21-32.
933 Ma W, Zhao X, Yin C, Jian F, Du X, *et al.* 2020. A chromosome-level genome assembly reveals
934 the genetic basis of cold tolerance in a notorious rice insect pest, *Chilo suppressalis*. Mol
935 Ecol Res. 20:268-282.
936 Ma X, Shao E, Chen W, Cotto-Rivera RO, Yang X, *et al*. 2022. Bt Cry1Ac resistance in
937 *Trichoplusia ni* is conferred by multi-gene mutations. Insect Biochem Mol Biol.
938 140:103678.
939 Magwene PM, Willis JH, Kelly JK. 2011. The statistics of bulk segregant analysis using next
940 generation sequencing. PLoS Comp Biol. 7:e1002255.
941 Mansfeld BN, Grumet R. 2018. QTLseqr: an R package for bulk segregant analysis with next-
942 generation sequencing. Plant Genom. 11:180006.
943 Marçais G, Delcher AL, Phillippy AM, Coston R, Salzberg SL, *et al.* 2018. MUMmer4: a fast
944 and versatile genome alignment system. PLoS Comp Biol. 14:e1005944.
945 Mathers TC. 2020. Improved genome assembly and annotation of the soybean aphid (*Aphis*
946 *glycines* Matsumura). G3 (Bethesda). 10: 899-906.
947 Musser FR, Catchot AL, Conley SP, Davis JA, DiFonzo C, *et al.* 2019. 2018 Soybean insect
948 losses in the United States. Midsouth Entomol. 12: 1-24.
949 National Academies of Sciences, Engineering, and Medicine. 2016. *Genetically Engineered*
950 *Crops: Experiences and Prospects*. Washington DC, National Academies Press.
951 Orpet RJ, Degain BA, Unnithan GC, Welch KL, Tabashnik BE, *et al.* 2015a. Effects of dietary
952 protein to carbohydrate ratio on Bt toxicity and fitness costs of resistance in *Helicoverpa*
953 *zea*. Entomol Exp Appl. 156:28-36.
954 Orpet RJ, Degain BA, Tabashnik BE, Carrière Y. 2015b. Balancing Bt toxin avoidance and
955 nutrient intake by *Helicoverpa zea* (Lepidoptera: Noctuidae) larvae. J Econ Entomol.
956 108:2581-2588.

957 Palmer JN, Stajich J. 2020. Funannotate v1.8.1: Eukaryotic genome annotation (v1.8.1). Zenodo.
958 https://doi.org/10.5281/zenodo.4054262.
959 Patro R, Duggal G, Love MI, Irizarry RA, Kingsford C. 2017. Salmon provides fast and bias-
960 aware quantification of transcript expression. Nat Meth. 14:417-419.
961 Pearce SL, Clarke DF, East PD, Elfekih S, Gordon KHJ, *et al.* 2017. Genomic innovations,
962 transcriptional plasticity and gene loss underlying the evolution and divergence of two
963 highly polyphagous and invasive *Helicoverpa* pest species. BMC Biol. 15:63.
964 Perera OP, Little NS, Abdelgaffar H, Jurat-Fuentes JL, Reddy GVP. 2021. Genetic knockouts
965 indicate that the ABCC2 protein in the bollworm *Helicoverpa zea* is not a major receptor
966 for the Cry1Ac insecticidal protein. Genes. 12:1522.
967 Pertea M, Pertea GM, Antonescu CM, Chang TC. Mendell JT, *et al.* 2015. StringTie enables
968 improved reconstruction of a transcriptome from RNA-seq reads. Nat Biotech. 33:290-
969 295.
970 Peterson B, Bezuidenhout CC, Van den Berg J. 2017. An overview of mechanisms of Cry toxin
971 resistance in lepidopteran insects. J Econ Entomol. 110:362-377.
972 Qin J, Guo L, Ye F, Kang S, Sun D, *et al.* 2021. MAPK-activated transcription factor PxJun
973 suppresses *PcABCB1* expression and confers resistance to *Bacillus thuringiensis* Cry1Ac
974 toxin in *Plutella xylostella* (L.). Appl Env Microbiol. 87:13.
975 Rajagopal R, Arora N, Sivakumar S, Rao NGV, Nimbalkar SA, *et al.* 2009. Resistance of
976 *Helicoverpa armigera* to Cry1Ac toxin from *Bacillus thuringiensis* is due to improper
977 processing of the protoxin. Biochem J. 419:309-316.
978 Rausch T, Fritz MH-Y, Untergasser A, Benes V. 2020. Tracy: basecalling, alignment, assembly
979 and deconvolution of sanger chromatogram trace files. BMC Genom. 21:230.
980 Reisig DD, Huseth AS, Bacheler JS, Aghaee M-A, Braswell L, *et al.* 2018. Long-term and
981 observational evidence of practical *Helicoverpa zea* resistance to cotton with pyramided
982 Bt toxins. J Econ Entomol. 111:1824-1833.
983 Reisig DD, DiFonzo C, Dively G, Fargan Y, Gore F, *et al.* 2021. Best management practices to
984 delay the evolution of Bt resistance in Lepidopteran pests without high susceptibility to
985 Bt toxins in North America. J Econ Entomol. https://doi.org/10.1093/jee/toab247.
986 Rimmer A, Phan H, Mathieson I, Iqbal Z, Twigg SRF, *et al.* 2014. Integrating mapping-,
987 assembly-, and haplotype-based approaches for calling variants in clinical sequencing

988 applications. Nat Genet. 46:912-918.
989 Roach MJ, Schmidt SA, Borneman AR. 2018. Purge Haplotigs: allelic contig reassignment for
990 third-gen diploid genome assemblies. BMC Bioinf. 19:460.
991 Robinson MD, McCarthy DJ, Smythe GK. 2010. edgeR: a Bioconductor package for differential
992 expression analysis of digital gene expression. Bioinformatics. 26:139-140.
993 Robinson JT, Thorvaldsdóttir H, Wenger AM, Zehir A, Mesirov JP. 2017. Variant review with
994 the Integrative Genomics Viewer. Cancer Res. 77:31-34.
995 Romeis J, Naranjo SE, Meissle M, Shelton AM. 2018. Genetically engineered crops help support
996 conservation biological control. Biol Contr. 130:136–154.
997 Schmidt H, Hellmann SL, Waldvogel A-M, Feldmeyer B, Hankeln T, *et al.* 2020. A high-quality
998 genome assembly from short and long reads for the non-biting midge *Chironomus*
999 *riparius* (Diptera). G3 (Bethesda). 10:1151-1157.
1000 Seppey M, Manni M, Zdobnov EM. 2019. BUSCO: assessing genome assembly and annotation
1001 completeness. In: Kollmar M (ed.) Gene Prediction. Methods in Molecular Biology, vol
1002 1962. Humana, New York, NY. pp. 227-245.
1003 Shen W, Le S, Li Y, Hu F. 2016. SeqKit: a cross-platform and ultrafast toolkit for FASTA/Q
1004 manipulation. PLoS One. 11:e0163962.
1005 Sievers F Higgins DG. 2018. Clustal Omega for making accurate alignments of many protein
1006 sequences. Prot Sci. 27:135-145.
1007 Singh U, Wurtele ES. 2021. orfipy: a fasta and flexible tool for extracting ORFs. Bioinformatics.
1008 37:3019-3020.
1009 Smit AFA, Hubley R, Green P. 2013-2015. RepeatMasker Open-4.0. http://repeatmasker.org
1010 Smith JL, Farhan Y, Schaafsma AW. 2019. Practical resistance of *Ostrinia nubilalis*
1011 (Lepidoptera: Crambidae) to Cry1F *Bacillus thuringiensis* maize discovered in Nova
1012 Scotia, Canada. Sci Rep. 9:18247.
1013 Soberón M, Pardo-López L, López I, Gómez I, Tabashnik BE, *et al.* 2007. Engineering modified
1014 Bt toxins to counter insect resistance. Science. 318:1640-1642.
1015 Soneson C, Love MI, Robinson MD. 2016. Differential analyses for RNA-seq: transcript-level
1016 estimates improve gene-level inferences. F100Research. 4:1521.
1017 Tabashnik BE and Carrière Y. 2019. Global patterns of resistance to Bt crops highlighting pink
1018 bollworm in the United States, China, and India. J Econ Entomol. 112:2513-2523.

1019 Tabashnik BE, Liu Y-B, Malvar T, Heckel DG, Masson L, *et al.* 1998. Insect resistance to
1020 *Bacillus thuringiensis*: uniform or diverse? Phil Trans R Soc B. 353:1751-1756.
1021 Tabashnik BE, Gassmann AJ, Crowder DW, Carrière Y. 2008. Insect resistance to Bt crops:
1022 evidence versus theory. Nat Biotech. 26:199-202.
1023 Tabashnik BE, Liesner LR, Ellsworth PC, Unnithan GC, Fabrick JA, *et al.* 2021. Genetically
1024 engineered cotton synergizes eradication of the pink bollworm a century after its invasion
1025 of the United States. Proc Natl Acad Sci USA. 118:e2019115118.
1026 Taylor KL, Hamby KA, DeYonke AM, Gould F, Fritz ML. 2021. Genome evolution in an
1027 agricultural pest following adoption of transgenic crops. Proc Natl Acad Sci USA.
1028 118:e2020853118.
1029 U.S. Dept. of Agriculture, Agricultural Marketing Service. Cotton Varieties Planted 2008 Crop.
1030 https://apps.ams.usda.gov/Cotton/AnnualCNMarketNewsReports/VarietiesPlanted/2008-
1031 VarietiesPlanted.pdf https://www.ams.usda.gov/mnreports/cnavar.pdf (accessed 3
1032 December 2021).
1033 U.S. Dept. of Agriculture, Economic Research Service. 2020. Adoption of Genetically
1034 Engineered Crops in the U.S. https://www.ers.usda.gov/data-products/adoption-of-
1035 genetically-engineered-crops-in-the-us/ (accessed 3 December 2021).
1036 Valencia-Montoya WA, Elfekih S, North HL, Meier JI, Warren IA, *et al.* 2020. Adaptive
1037 introgression across semipermeable species boundaries between local *Helicoverpa zea*
1038 and invasive *Helicoverpa armigera* moths. Mol Biol Evol. 37:2568-2583.
1039 Walker BJ, Abeel T, Shea T, Priest M, Abouelliel A, *et al.* 2014. Pilon: an integrated tool for
1040 comprehensive microbial variant detection and genome assembly improvement. PLoS
1041 One. 9:e112963.
1042 Wan F, Yin C, Tang R, Chen M, Wu Q, *et al.* 2019. A chromosome-level genome assembly of
1043 *Cydia pomonella* provides insights into chemical ecology and insecticide resistance. Nat
1044 Commun. 10:4237.
1045 Wang B, Wei J, Wang Y, Chen L, Liang G. 2020. Polycalin is involved in the toxicity and
1046 resistance to Cry1Ac toxin in *Helicoverpa zea*. Arch Ins Biochem Physiol. 104:e21661.
1047 Ward CM, Perry KD, Baker G, Powis K, Heckel DG, *et al.* 2021. A haploid diamondback moth
1048 (*Plutella xylostella* L.) genome assembly resolves 31 chromosomes and identifies a
1049 diamide resistance mutation. Ins Biochem Mol Biol. 138:103622.

1050 Watters JW, Dewar K, Lehoczky J, Boyartchuk V, Dietrich WF. 2001. Kif1C, a kinesin-like
1051 motor protein, mediates mouse macrophage resistance to anthrax lethal factor. Curr Biol.
1052 11: 1503-1511.
1053 Welch KL, Unnithan GC, Degain BA, Wei J, Zhang J, *et al.* 2015. Cross-resistance to toxins
1054 used in pyramided Bt crops and resistance to Bt sprays in *Helicoverpa zea*. J Invert
1055 Pathol. 132:149-156.
1056 Welter D, MacArthur J, Morales J, Burdett T, Hall P, *et al.* 2014. The NHGRI GWAS Catalog, a
1057 curated resource of SNP-trait associations. Nuc Ac Res. 42:D1001-D1006.
1058 Xu H, Zhao X, Yang Y, Chen X, Mei Y, *et al.* 2021. Chromosome-level genome assembly of an
1059 agricultural pest, the rice leaffolder *Cnaphalocrocis exigua* (Crambidae, Lepidoptera).
1060 Mol Ecol Res. 21:561-572.
1061 Yan B, Ou H, Wei L, Wang X, Yu X, *et al.* 2021. A chromosome-level genome assembly of
1062 *Ephestia elutella* (Hübner, 1796) (Lepidoptera: Pyralidae). Genom Biol Evol.
1063 13:evab114.
1064 Ye C, Ma ZS. 2016. Sparc: a sparsity-based consensus algorithm for long erroneous sequencing
1065 reads. PeerJ. 4:e2016.
1066 Ye C, Hill CM, Wu S, Ruan J, Ma ZS. 2016. DBG2OLC: efficient assembly of large genomes
1067 using long erroneous reads of the third generation sequencing technologies. Sci Rep.
1068 6:31900.
1069 Yoder AD, Tiley GP. 2021. The challenge and promise of estimating the de novo mutation rate
1070 from whole-genome comparisons among closely related individuals. Mol Ecol. 30:6087–
1071 6100.
1072 Yu W, Lin S, Dimase M, Niu Y, Brown S, *et al.* 2021. Extended investigation of field-evolved
1073 resistance of the corn earworm *Helicoverpa zea* (Lepidoptera: Noctuidae) to *Bacillus*
1074 *thuringiensis* Cry1A.105 and Cry2Ab2 proteins in the southeastern United States. J Inv
1075 Pathol. 183: 107560
1076 Zhang S, Cheng H, Gao Y, Wang G, Liang G, *et al.* 2009. Mutation of an aminopeptidase N
1077 gene is associated with *Helicoverpa armigera* resistance to *Bacillus thuringiensis* Cry1Ac
1078 toxin. Ins Biochem Mol Biol. 39:421-429.
1079 Zhang M, Wei J, Ni X, Zhang J, Jurat-Fuentes JL, *et al.* 2019a. Decreased Cry1Ac activation by
1080 midgut proteases associated with Cry1Ac resistance in *Helicoverpa zea*. Pest Man Sci.

75:1099-1106.

Zhang S, Gu S, Ni X, Li X. 2019b. Genome size reversely correlates with host plant range in *Helicoverpa* species. Front Physiol. 10:29.

Zhang S, Shen S, Peng J, Zhou X, Kong X, *et al.* 2020. Chromosome-level genome assembly of an important pine defoliator, *Dendrolimus punctatus* (Lepidoptera; Lasiocampidae). Mol Ecol Res. 20:1023-1037.

Zhao S, Jiang D, Wang F, Tabashnik BE, Wu Y. 2021. Independent and synergistic effects of knocking out two ABC transporter genes on resistance to *Bacillus thuringiensis* toxins Cry1Ac and Cry1Fa in diamondback moth. Toxins. 13:9.

1092 **Table 1** Genotype and allele frequencies at 12 markers on the chromosome 13 QTL for resistant
1093 and susceptible GA-RS larvae from generations F22 and F23.
1094

Marker	Bp (Chr13)	Resistant larvae		Susceptible larvae		
		Genotypes (GG / GL / LL)[a]	G allele frequency	Genotypes (GG / GL / LL)[a]	G allele frequency	*P-value*[b]
1	4,110,560	41 / 15 / 4	0.81	23 / 23 / 3	0.70	1.0
2	4,281,434	30 / 23 / 7	0.69	9 / 24 / 16	0.43	9.6 e-03
3	4,379,538	41 / 18 / 1	0.83	13 / 24 / 12	0.51	2.4 e-04
4	4,475,706	40 / 17 / 0	0.85	13 / 24 / 12	0.51	4.0 e-05
5	4,596,970	43 / 17 / 0	0.86	13 / 24 / 12	0.51	3.0 e-05
6	4,720,567	39 / 17 / 2	0.82	12 / 13 / 12	0.50	1.3 e-04
7	4,829,519	40 / 18 / 1	0.83	13 / 23 / 13	0.50	1.0 e-04
8	4,902,478	38 / 21 / 1	0.81	13 / 23 / 13	0.50	1.0 e-04
9	4,998,799	38 / 19 / 1	0.82	12 / 23 / 14	0.48	5.0 e-05
10	5,226,319	27 / 19 / 3	0.75	14 / 24 / 5	0.61	0.47
11	5,727,295	11 / 22 / 7	0.55	5 / 14 / 1	0.60	0.29
12	6,232,397	15 / 19 / 8	0.58	3 / 33 / 8	0.44	1.0

[a] G indicates the allele was more common in the resistant GA-R strain,
L indicates the allele was more common in the susceptible LAB-S strain.
[b] From Fisher's exact test of the null hypothesis that allele frequency did not differ between the resistant and susceptible larvae.

1095

Table 2 Larval midgut expression of genes in the region of chromosome 13 QTL associated with resistance to Cry1Ac.

Gene ID	Start - Stop (orientation)	Name	Larval midgut expression (mean $\log_2$ CPM)
MSTRG.8092	4,371,598 – 4,491,148 (+)	*Cyclic AMP-response element-binding protein A*	2.44
MSTRG.8095	4,491,241 – 4,520,601 (-)	*Heparan-alpha-glucosaminide-N-acetyltransferase*	-0.02*
MSTRG.8097	4,504,492 – 4,507,681 (+)	*Juvenile hormone esterase-like Carboxyl/cholinesterase CCE006D*	4.84
hz_G0000107	4,536,278 – 4,541,251 (+)	*Lipase member H-B-like*	N/A
MSTRG.8100	4,541,250 – 4,593,328 (-)	*Phosphatidylinositol 4-phosphate 3-kinase C2 domain-containing subunit alpha*	3.25
MSTRG.8101	4,546,116 – 4,547,856 (+)	*Kinesin-related protein 12-like*	7.08
hz_G0000111	4,593,482 – 4,595,264 (-)	Uncharacterized protein	N/A
hz_G0000112	4,600,520 – 4,606,939 (+)	Uncharacterized protein	N/A
MSTRG.8102	4,607,861 – 4,617,975 (-)	*Ubiquitin-protein ligase E3A*	3.88
MSTRG.8103	4,618,419 – 4,620,800 (+)	*Retinal rod rhodopsin-sensitive cGMP 3`, 5`-cyclic phosphodiesterase subunit delta*	2.98

Gene IDs refer to the StringTie annotation when expressed for correspondence with the RNA-seq data. Funannotate IDs refer to non-expressed genes. N/A indicates the gene was not expressed. *Because of the low expression of this gene (12-fold lower than the median for the other six expressed genes), we considered it not to be substantially expressed.

Table 3 GWAS and RNA-seq results for 11 genes previously implicated in lepidopteran resistance to Cry1Ac.

Gene	Key reference	*H. zea* genome location[a]	Gene ID[b]	GWAS: *P*-value[c]	RNA-seq: GA-R vs. LAB-S *P*-value[d]	RNA-seq: GG vs. LL *P*-value[d]
ABCC1	Chen *et al.* 2019a	12: 9.24-9.29	7445	0.16	**0.0014**	0.29
ABCC2	Baxter *et al.* 2011	15: 7.07-7.09	9800	0.35	0.95	0.56
APN1	Zhang *et al.* 2009	9: 11.33-11.37	5943	0.53	0.32	0.33
Cadherin	Gahan *et al.* 2001	6: 1.89-1.97	4086	0.46	1.0	0.13
Cadherin-86C	Fritz *et al.* 2020	12: 4.60-4.62	7702	0.49	0.69	0.75
MAPK4	Guo *et al.* 2015	12: 6.80-6.82	9824	0.21	0.12	0.43
mALP	Jurat-Fuentes *et al.* 2011	8: 10.41-10.43	4895	0.37	0.11	0.62
Polycalin	Wang *et al.* 2020	25: 2.72-2.73	16287	0.48	0.73	0.14
SP2	Rajagopal *et al.* 2009	7: 1.34-1.35	4260	0.53	0.85	0.88
Tetraspanin1	Jin *et al.* 2018	10: 11.58-11.59	6160	0.087	0.061	0.20
TryR	Liu *et al.* 2014	27: 2.04-2.09	17235	0.60	0.97	1.0

[a] Chromosome: Mb

[b] Full Gene ID begins with MSTRG.

[c] Lowest *P*-value for any SNP in the gene based on the G' analysis

[d] *P*-values are FDR-corrected, bold indicates significant at < 0.05.

Figure 1 Manhattan plot of GWAS results showing $-\log_{10}$ of the *P*-values for Z-scores comparing allele frequencies between resistant and susceptible larvae. The red line indicates the threshold for significant association ($P = 5e^{-8}$).

Figure 2 Association between resistance to Cry1Ac and SNPs within the chromosome 13 QTL. (A) Proportion of significant SNPs ($P < 1e^{-5}$) from the Z-score analysis of the QTL data in 10-kb sliding windows. The horizontal red line indicates the 95th percentile of the distribution. (B) Evidence of a selective sweep in GA-R from Tajima's D in 50-kb sliding windows. Blue shading covers the QTL from 4.37 to 4.62 Mb. The vertical red bars show the locations of markers 4 and 5 (Table 1). The red asterisk indicates the location of *kinesin-12*.

Figure 3 Ten genes including *kinesin-12* in the resistance-associated QTL on chromosome 13. (A) The four genes at the top are in the (–) orientation, the other six below are in the (+) orientation (Table 2). The four genes in white were not expressed substantially in the midgut. Darker red indicates higher expression in the midgut (Table 2). (B) The structure of *kinesin-12* in LAB-S and GA-R. Boxes represent exons, light blue indicates UTRs, and dark blue signifies coding regions.

Figure 4 Survival of the heterogeneous GA-RS strain of *H. zea* tested on diet with 1 (red) or 10 (blue) µg Cry1Ac per cm^2 diet. Survival at each test concentration decreased significantly. Regressions of percent survival to third instar on generation: $y = -2.49x + 88.63$, $R^2 = 0.94$, df = 2, $P = 0.021$ and $y = -0.36x + 11.67$, $R^2 = 0.91$, df = 3, $P = 0.0074$ for 1 and 10 µg Cry1Ac per cm^2 diet, respectively. Generation 26 was tested only at the higher concentration. Shaded areas show 95% confidence intervals.

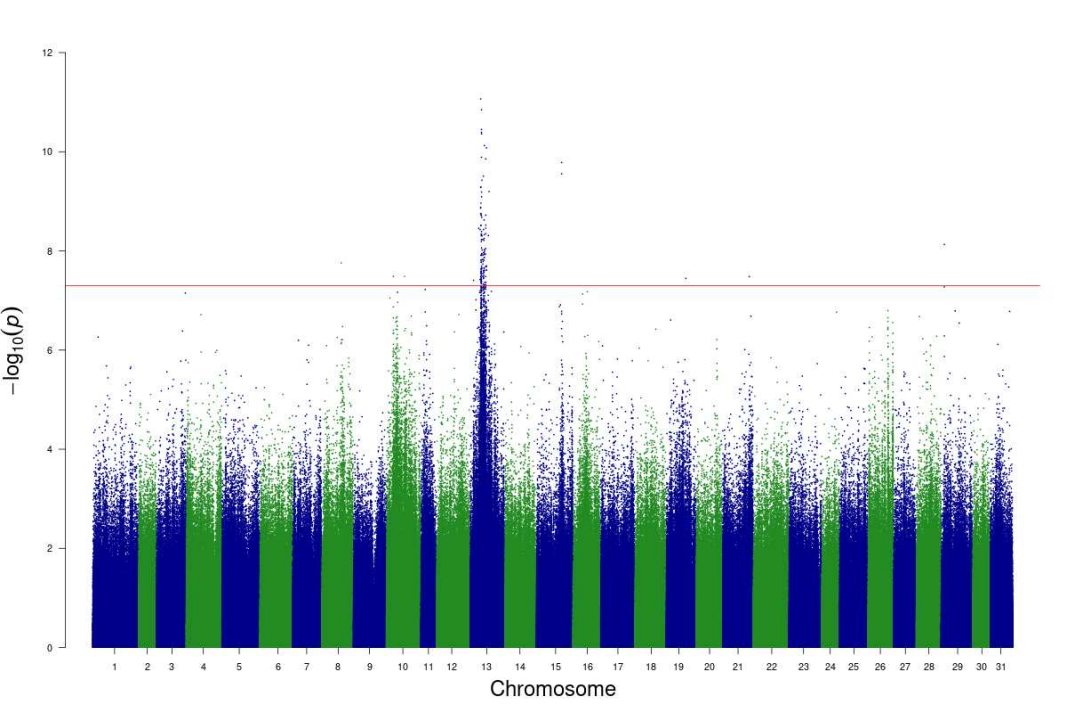
12
10
8
6
4
2
0
$-\log_{10}(p)$
1 2 3 4 5 6 7 8 9 10 11 12 13 14 15 16 17 18 19 20 21 22 23 24 25 26 27 28 29 30 31
Chromosome

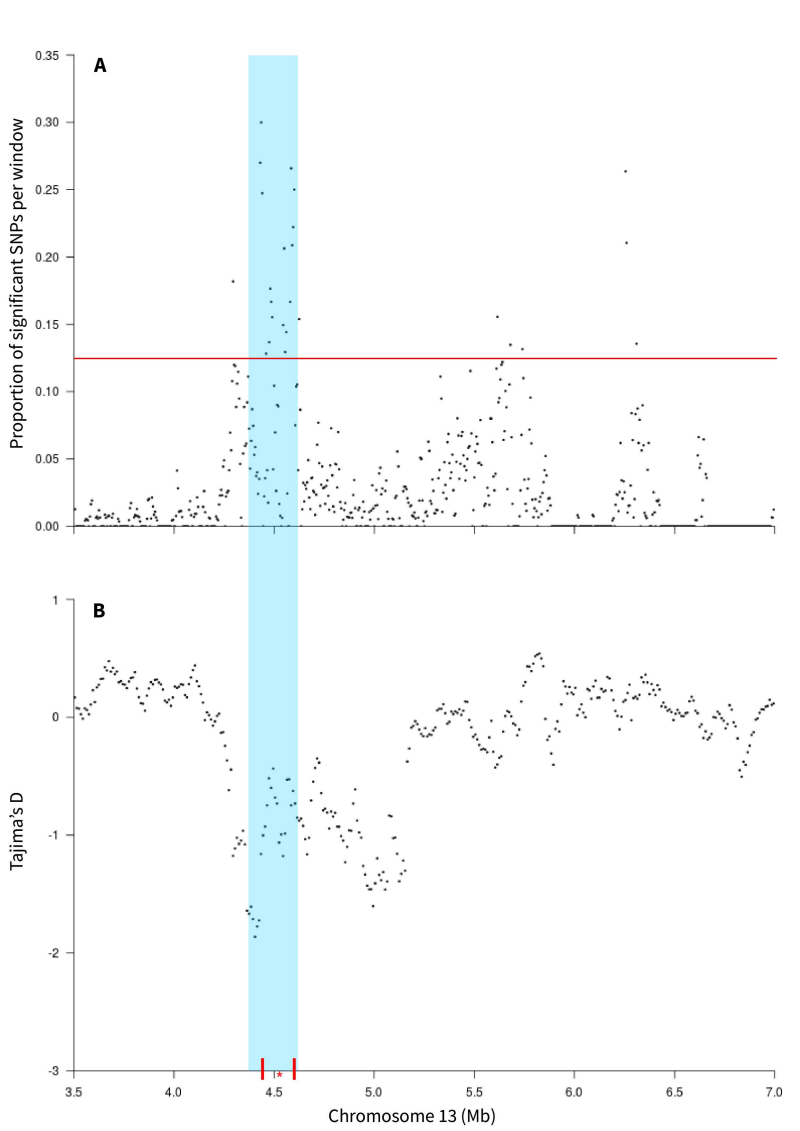
A
Proportion of significant SNPs per window
0.35
0.30
0.25
0.20
0.15
0.10
0.05
0.00
B
Tajima's D
1
0
-1
-2
-3
3.5
4.0
4.5
5.0
5.5
6.0
6.5
7.0
Chromosome 13 (Mb)

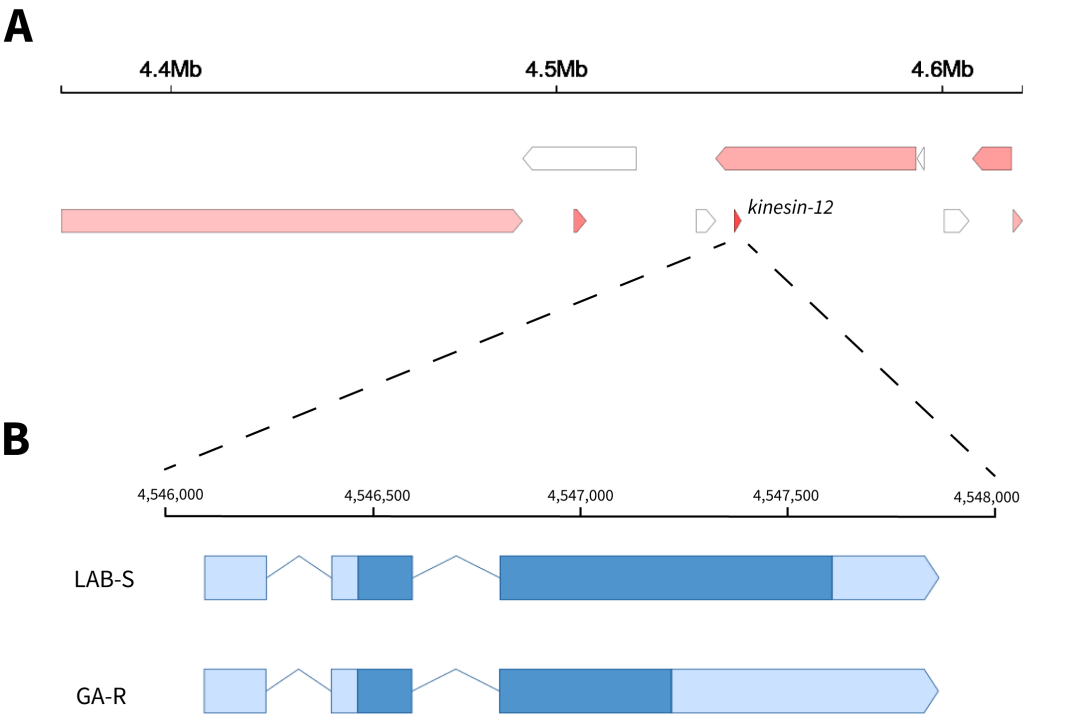
A
4.4Mb
4.5Mb
4.6Mb
kinesin-12
B
4,546,000
4,546,500
4,547,000
4,547,500
4,548,000
LAB-S
GA-R

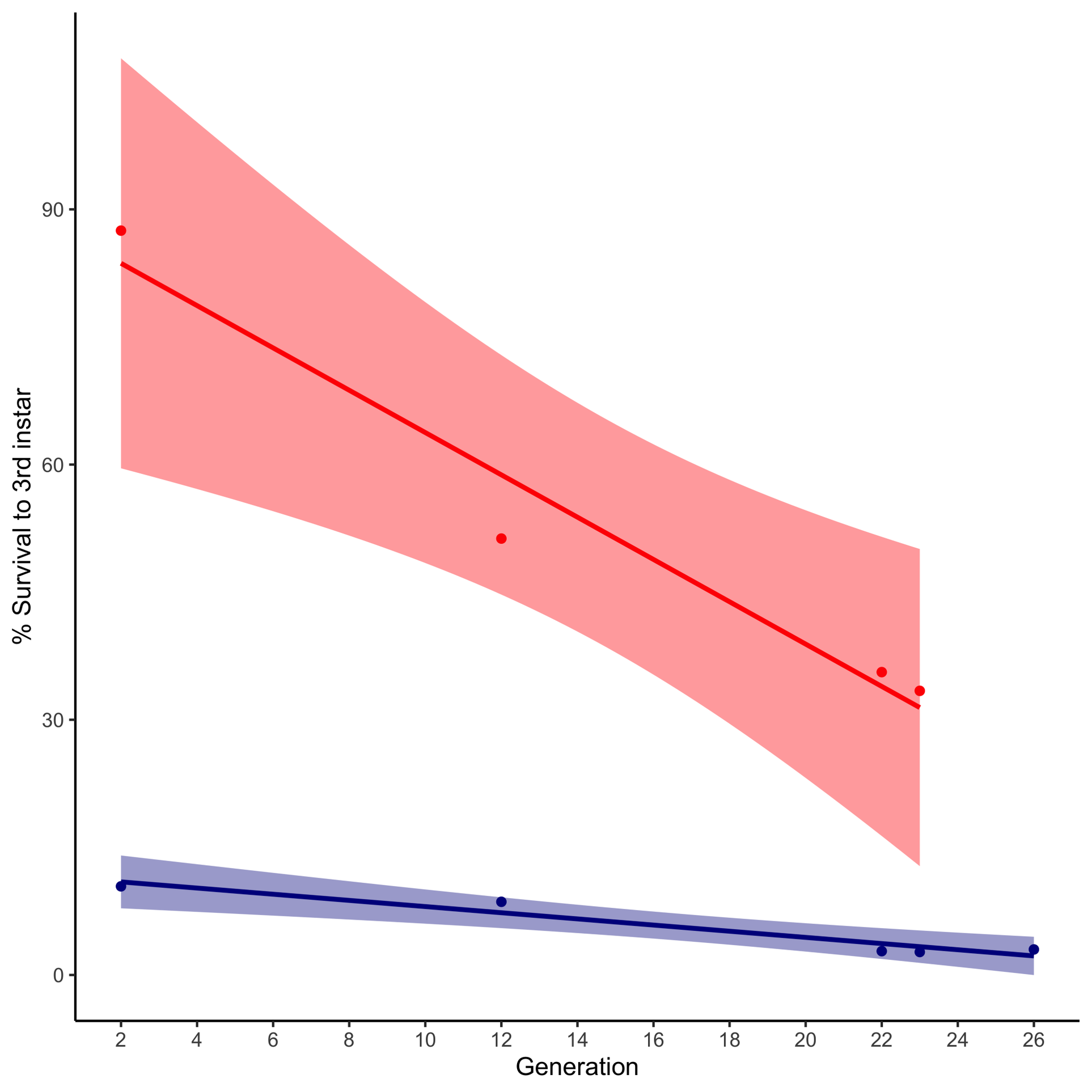
% Survival to 3rd instar
90
60
30
0
2
4
6
8
10
12
14
16
18
20
22
24
26
Generation